Full configuration interaction calculation of BeH adiabatic states

J. Pitarch-Ruiz,[1] J. Sánchez-Marin,[1,a)] A. M. Velasco,[2] and I. Martin[2]
[1]*Institut de Ciència Molecular, Universitat de València, Edifici d'Instituts Campus de Paterna, E-46980 Valencia, Spain*
[2]*Departamento de Química Física y Químíca Inorgánica, Facultad de Ciencias, Universidad de Valladolid, E-47005 Valladolid, Spain*

(Received 28 April 2008; accepted 11 June 2008; published online 6 August 2008)

An all-electron full configuration interaction (FCI) calculation of the adiabatic potential energy curves of some of the lower states of BeH molecule is presented. A moderately large ANO basis set of atomic natural orbitals (ANO) augmented with Rydberg functions has been used in order to describe the valence and Rydberg states and their interactions. The Rydberg set of ANOs has been placed on the Be at all bond distances. So, the basis set can be described as $4s3p2d1f/3s2p1d$(Be/H)+$4s4p2d$(Be). The dipole moments of several states and transition dipole strengths from the ground state are also reported as a function of the $R_{\mathrm{Be-H}}$ distance. The position and the number of states involved in several avoided crossings present in this system have been discussed. Spectroscopic parameters have been calculated from a number of the vibrational states that result from the adiabatic curves except for some states in which this would be completely nonsense, as it is the case for the very distorted curves of the $3s$ and $3p\ ^2\Sigma^+$ states or the double-well potential of the $4p\ ^2\Pi$ state. The so-called "D complex" at 54 050 cm^{-1} (185.0 nm) is resolved into the three $3d$ substates ($^2\Sigma^+, ^2\Pi, ^2\Delta$). A diexcited valence state is calculated as the lowest state of $^2\Sigma^-$ symmetry and its spectroscopic parameters are reported, as well as those of the $2\ ^2\Delta$ ($4d$) state The adiabatic curve of the $4\ ^2\Sigma^+$ state shows a swallow well at large distances (around 4.1 Å) as a result of an avoided crossing with the $3\ ^2\Sigma^+$ state. The probability that some vibrational levels of this well could be populated is discussed within an approached Landau–Zerner model and is found to be high. No evidence is found of the $E(4s\sigma)\ ^2\Sigma^+$ state in the region of the "D complex". Instead, the spectroscopic properties obtained from the $(4s\sigma)\ 6\ ^2\Sigma^+$ adiabatic curve of the present work seem to agree with those of the experimental $F(4p\sigma)\ ^2\Sigma^+$ state. The FCI calculations provide benchmark results for other correlation models for the open-shell BeH system and evidence both the limitations and capabilities of the basis set. © *2008 American Institute of Physics*. [DOI: 10.1063/1.2953584]

I. INTRODUCTION

A continued effort is being done to develop and improve theoretical methods of high quality for the calculations of electronic excitation energies[1–4] and well adapted for calculation in large systems and at geometries far from equilibrium. Most of these methods face the difficulties by means of multireference (MR) approaches [e.g., multireference configuration interaction (CI) more or less corrected for size-consistency error effects[5–11] or multireference perturbation theory[12–15]]. The extension of the single-reference configurations interaction (SR-CI) to the MR case is conceptually straightforward. However, because of the rapidly increasing size of the hamiltonian matrices, these approaches are commonly restricted to single and double (SD) excitations out of the chosen model space (MR-SDCI). Consequently, the so-called static and nondynamic correlation effects are to some extent taken into account efficiently, but, generally, there is an incomplete consideration of the multitude of higher than double hole-particle substitutions that contribute to the dynamic correlation. Multireference formulations can also be conceived for the approaches based in the coupled-cluster (CC) formulation.[3,16–23] However, the generalization of the SR-CC ansatz to the MR case is not unambiguous,[24,25] and, also, the resulting formalisms for all genuine MR-CC approaches are computationally very demanding. Moreover, some of the approximate methods yield excellent results in the neighborhood of the equilibrium geometry, but, unfortunately, breaks down entirely when dissociating the molecule into open-shell fragments (Ref. 26 and references therein). The extension of the approximate methods to general open-shell systems offers additional challenges related, in most cases, to the optimal selection of the one-electron basis, and in some cases is demanding, both theoretically and computationally.[24,25,27–32]

Full configuration interaction (FCI) calculations are very appealing because they are free of a number of formal disadvantages that affect approximate methods which truncate the space of excitations. Within the limits imposed by the Born–Oppenheimer (BO) approximation and the choice of the one-particle functions basis, FCI provides nonrelativistic exact results. Of course, only basis set of comparatively reduced size can be used and only systems with small number of electrons are eligible for a systematic FCI study. However, on the other hand, the results from such a study provide durable benchmarks for approximate methods.

a)Electronic mail: jose.sanchez@uv.es.

Among the first-row diatomic hydrides, BeH presents some special features that motivate its study. BeH molecule has been less analyzed experimentally than other hydrides, probably because of the toxicity related to the beryllium-containing compounds.[33] Colin and co-workers[34–45] have reported experimental data of the complex spectrum of a number of excited states of BeH but the list of experimental spectroscopic parameters appears still as mostly sparse.[46] Recorded detailed data are mainly related to the lowest states ($X\,^2\Sigma^+$, $A\,^2\Pi$, $C\,^2\Sigma^+$),[39,42–45] although absorption spectra involving some Rydberg states have also been analyzed in the past.[36,41]

The bond formation of BeH, both in ground state (GS) and excited states, deserve special interest, as many other compound of Be do, due to the relevance of the promotion from the $2s$ to the $2p$ orbital in the formation of the molecule. The Be($2p$) orbital contributes to the 2σ and 3σ molecular orbitals (MOs). This contribution is greater near the equilibrium geometry and decreases when the bond is stretched. However, at large distances the 2σ and 3σ MOs change in nature and this fact plays an important role in the dissociation of some states. Several avoided crossings of different nature (either valence-Rydberg mixing or ion-pair interaction[47,48]) become apparent and offer a variety of challenges to approached methods that would try to reproduce the potential energy curves along the whole domain of bond distances. Several works that have dealt with the low-lying states of BeH describe the important mixings in either the $^2\Pi$ or the $^2\Sigma^+$ states.[26,41,47–59]

BeH offer other properties that make it a good choice for a comprehensive FCI study. Apart from the above mentioned avoided crossings, we can mention its open-shell nature, the possible occurrence of featured potential wells at large R values (e.g., the controversial double-well nature related to the so-called $G\,^2\Pi$ state or the properties associated to the existence of a second minimum in the potential curve of the $B\,^2\Pi$ state[52]), the problem of the position of the $(4s\sigma)^2\Sigma^+$ state (theoretically predicted[47,53] as lying at higher energy than the $(3d)D$ state, which does not agree with reported experimental values[36]), not to mention the rather uncommon fact of a single chemical bond dissociating into a neutral closed-shell atom of just four electrons. Special attention deserves the interactions involving the valence state $C\,^2\Sigma^+$. This state affects by predissociation all the $^2\Sigma^+$ states and the Π^+ component of all the $^2\Pi$ states that it crosses (this causes, for example, the absence of the $(3s\sigma)^2\Sigma^+$ and $(3p\sigma)^2\Sigma^+$ states from the absorption spectrum and either broadening or missing groups of lines in the R and P branches of the $(4p\sigma)F\,^2\Sigma^+$ and $(3p\pi)B\,^2\Pi$ states).[36,37,41]

Early calculations by Bagus *et al.*[49] and Larsson[57] had reported the presence of a potential maximum in the $X\,^2\Sigma^+$ associated to the occurrence of a doublet instability[60,61] that produces two solutions at the ROHF step that cross and coexist in a finite region near $R=1.8R_e$ ($\sim$2.3 Å).[26,59,62] This is a good example of how methods based on single-reference wave functions can face challenging problems in following the potential curves even for the lowest states as $X\,^2\Sigma^+$ and $A\,^2\Pi$,[59] because the SCF wave functions do not dissociate properly to the appropriate states of the separated Be and H atoms.

Previous theoretical works that have calculated potential curves of several excited states on BeH are based on different approaches. Let us mention the early 1σ-frozen-core full CI by Henriet and Verhaegen,[47] the MRD-CI calculations by Petsalakis *et al.*,[48,53] and the MR-CI calculations by Machado *et al.*[52] As mentioned above, important nonadiabatic effects are present in this light molecule.[47,48,51,53,63–65] A recent work by Bubin and Adamowicz[66] reports non-Born–Oppenheimer variational calculations on the GS of the BeH system. Works which do not assume the BO approximation are very scarce. However, even if one remains in the BO approximation it is very important to have at disposal accurate adiabatic potential curves. Although some of the quoted works perform "*a posteriori*" diabatic or quasidiabatic coupling,[47,48,53] the need of good quality adiabatic descriptions cannot be ignored.[51]

The vibrational properties related to the adiabatic curves have been studied with some detail in the present work. Notwithstanding, the reader must keep in mind that these calculations assume separability between electronic and nuclear movements, but the energies strongly change upon diabatization and the spectroscopic properties should be consistently affected in nonadiabatic studies.

In a recent work[67] some of the authors have performed FCI calculations at the GS equilibrium distance in order to explore a large manifold of excited states of BeH, whose vertical excitation energies, the electric dipole and quadrupole moments and their transition counterparts were calculated. In the present paper the calculation deal with a smaller set of low-lying states of BeH, including the lower Rydberg states, as a function of the Be–H distance. A basis set slightly larger can be used in both the valence and the Rydberg subsets of basis functions.

In Sec. II, the details of the calculation referred to the basis set, the FCI calculation itself, the calculation of the spectroscopic parameters and the preliminary study of the GS are outlined. The adiabatic curves and related results are shown and discussed in Sec. III. They are grouped in subsections concerning the adiabatic curves, the atomic asymptotes, the nature of the adiabatic states and their avoided crossings, and the spectroscopic parameters. Two subsections of Sec. III are devoted to the dipole moments and transition dipole moments from the GS. Another one pays special attention to the long-distance minimum in the $4\,^2\Sigma^+$ state. Conclusions are summarized in Sec. IV.

II. DETAILS OF THE CALCULATIONS

A. Basis set description

The basis set used for the calculation of the adiabatic curves in this work is made of atomic natural orbitals, ANOs, as described by Widmark *et al.*[68] The basis set consists of a *valence set* augmented with a one-center series of increasingly diffuse ANOs that will be denoted as *Rydberg AOs*. This basis set can be described as $4s3p2d1f/3s2p1d$(Be/H)+$4s4p2d$(Be) because the aug-

TABLE I. Exponents and coefficients for the ANO Rydberg functions set of BeH.

Exponents	Coefficients			
		s functions		
0.024 624	0.428 296 23	−0.660 574 15	1.556 113 91	−2.879 415 49
0.011 253	0.630 160 84	−0.613 324 75	−1.447 074 66	6.630 312 80
0.005 858	−0.189 522 36	0.995 255 40	−0.590 539 38	−5.633 700 69
0.003 346	0.411 576 35	0.310 724 61	−1.056 127 51	3.103 051 50
0.002 048	−0.502 555 48	0.507 711 47	2.444 996 72	−5.823 314 24
0.001 324	0.423 334 88	−0.377 568 65	−0.771 647 80	6.574 402 03
0.000 893	−0.224 902 59	0.201 228 02	0.606 301 07	−2.650 393 28
0.000 624	0.055 673 24	−0.051 999 86	−0.142 611 51	0.770 669 90
		p functions		
0.042 335	0.037 292 72	−0.499 587 41	0.608 468 89	−0.664 467 92
0.019 254	0.318 526 38	−0.598 883 88	0.290 549 47	0.227 943 72
0.009 988	0.413 411 41	0.197 831 63	−0.982 894 19	1.116 630 96
0.005 689	0.304 442 33	0.412 512 56	−0.648 841 15	0.061 660 70
0.003 476	−0.017 656 30	0.329 281 71	0.671 657 05	−2.022 239 90
0.002 242	0.045 122 29	0.067 474 44	0.609 392 05	0.041 065 21
0.001 511	−0.029 407 88	0.039 712 12	0.167 137 09	0.542 405 97
0.001 055	0.008 375 40	−0.015 103 62	0.040 054 27	0.962 946 85
		d functions		
0.060 540	0.156 698 15	−0.255 320 67		
0.027 446	0.298 161 46	−0.295 661 39		
0.014 204	0.407 320 63	−0.229 369 75		
0.008 077	0.200 665 70	0.245 922 31		
0.004 927	0.128 397 31	0.311 901 45		
0.003 175	−0.042 769 19	0.450 747 40		
0.002 137	0.030 886 45	0.057 566 73		
0.001 491	−0.009 155 99	0.029 156 54		

mentation series of Rydberg AOs is unique and always centered in the Be nucleus. This choice deserves some comments that will be discussed below, in Sec. II E. The Rydberg AOs subset has been generated at a single point (R=1.327 Å) that corresponds to the equilibrium distance of the ground state (GS) as obtained from the *valence set*. The procedure proposed by Roos *et al.*[69] has been followed in the way described elsewhere.[67] The universal optimized exponents of Kaufmann *et al.*[70] are used as a single set of exponents common to all the unsegmented Rydberg ANO functions for each ℓ value. This type of basis sets has proven reliable for the calculation of vertical excitation energies (VEEs) in a number of cases that involved Rydberg states.[67,71–75] The basis set here described will be denoted as ANO1+4*s*4*p*2*d* when necessary. The 4*s*4*p*2*d* Rydberg AOs are reported in Table I. A few calculations of the GS potential have been performed with some other basis sets,[68,76–79] as reported in Sec. II E.

B. Programs

The SCF procedure, property-integral calculation, and bielectronic-integral transformations have been performed with the MOLCAS code.[80] The FCI calculations of energy and electrical properties have been performed with the VEGA code.[81,82] The interested reader can find the most relevant details of the multiroot convergence procedure elsewhere.[67] An interface program is required to convert MOLCAS property-integral files to a format suitable for the VEGA program.[83–88] Other codes such as Wolfram's MATHEMATICA,[89] Hutson's CDIST,[90,91] and Le Roy's LEVEL8.0 (Ref. 92) have been used for auxiliary calculations and data treatment as it is described in Secs. II C, II D, and III D.

C. FCI calculations and computational aspects

All the calculations have been performed in the abelian C_{2v} group, whose irreducible representations are reported hereafter in the order (a_1,b_1,b_2,a_2). The one-electron molecular basis has been obtained with the self-consistent field, SCF, procedure as it is implemented in the MOLCAS suite for single-reference open-shell systems, after placing the five electrons in the first three MOs of a_1 symmetry (i.e., $1a_1^2 2a_1^2 3a_1^1$ that correlates with $1\sigma^2 2\sigma^2 3\sigma^1$ in $C_{\infty v}$). No post-SCF adaptation of the MO has been carried out. In the case that a conventional reference for the correlation energy is desired, the univocally defined (1e-1MO)-CASSCF value associated to the ANO1+4*s*4*p*2*d* basis set at R_e=2.494 43a_0 (1.320 Å) can be used. It amounts to −15.152 877 68 a.u. Each single-point FCI calculation in the C_{2v} symmetry with the ANO1+4*s*4*p*2*d* basis set involved 70 MOs (32, 16, 16, 6) and 5 electrons. The half-filled highest-energy occupied molecular orbital (HOMO) 3σ orbital will be denoted as singly occupied MO (SOMO). Hence, the 2σ MO will be denoted as HOMO-1 when convenient for discussions. The FCI matrices in the C_{2v} representations involve 33 357 248, 33 048 544, 33 048 544, and 32 742 764 Slater determinants. The adiabatic potential energy curves of seven (in some regions nine) A_1 states, seven B_1 and B_2 states, and five A_2 states have been calculated. The molecular axis is the x axis. This work focuses on the lower $^2\Sigma^+$ ($^2A_1$), $^2\Delta$ ($^2A_1$ and $^2A_2$) and $^2\Pi$ ($^2B_1$ and $^2B_2$) states. We also tried to converge onto roots of some additional higher-energy states, that are not reported here. This is helpful because the calculations are stopped, at each point, once these higher states attain a convergence in their energy of 10^{-7} a.u. In this way, a better convergence (normally lower than 10^{-9}–10^{-10} a.u.) is reached for the states of interest. Besides this, the features of the potential curves that could result from interactions with states lying on top of them can be considered as more reliably determined. The duplication of the calculations in some of the degenerate states (B_1 and B_2 for Π states or A_1 and A_2 for Δ states) have provided additional test on the reliability of the calculations and of the symmetry assignments for Δ and Σ^+ states.

The FCI dipole matrix elements have been computed, into the dipole length approach, by means of a scalar product in the FCI space between the representative vector of each excited state $|\text{exc}\rangle$ and that of either $\hat{\mu}|0\rangle$ or $\hat{\mu}|\text{exc}\rangle$, where $\hat{\mu}$ represents the desired dipole component operator and $|0\rangle$ the GS eigenvector. The square of the electronic transition moment gives the transition dipole strength (TDS), $|\langle\text{exc}|\hat{\mu}|0\rangle|^2$. The total molecular electric dipole moment values are obtained at each point after adding the nuclear contributions in the point charge model. As the origin is placed on Be, this quantity just amounts to $+R$ a.u.

D. Spectroscopic parameters and its accuracy

Compiling the spectroscopic parameters for different molecules and states is a common practice that is widely recognized as convenient and practical[93,94] for comparing, in the easiest way, energy potentials and rotation-vibration properties. A given calculated (say, e.g., adiabatic) potential curve can be directly compared with another one, that is taken as benchmark reference, by comparing the vibrational term values $G(v)$ or the vibration-rotation ones, $G_{v,J}$ after assuming vibration-rotation separability. These values can be obtained from the numerical solution of the one-dimensional Schrödinger equation for each $V(R)$ calculated in the framework of the Born–Oppenheimer approach. Better approaches can be used,[45,95] but this is enough for the purpose of the present work. The wave function associated to each G_v level allows to get the B_v rotational constants associated to the vibrational state v from the expected value of $1/R^2$, so that the B_v values can be also compiled for each state. Along the present work, the symbol G is kept to denote energy levels reported in wave number units. Only ground state rotational states for each v have been considered, so that the symbol J is used here to denote a generic rotational quantum number and no attention is paid to the Hund's coupling cases.

The $G(v)$ and B_v values have been obtained for bound states using a revised version of Hutson's CDIST program.[90,91] The reliability of the results for low v values was assessed for a few states against the same property values calculated with Le Roy's LEVEL8.0 code.[92] The spectroscopic parameters and molecular constants [R_e, D_e (dissociation energy), B_e, α_e, ω_e, $\omega_e x_e$, $\omega_e y_e$] are reported for each state, instead of just providing the $G(v)=G_{v,J=0}$ and B_v values. The main drawback in doing so comes, most likely, from the sensitivity of the values of these constants to the conditions of each actual calculation. It is not surprising that the number of vibrational terms $G(v)$ used to fit, e.g., the $(\omega_e, \omega_e x_e, \omega_e y_e)$ set, influences the results in a non-negligible way (with differences in ω_e, sometimes, of tens of wave numbers), even for well behaved potentials showing Morse-type behavior all along the curve. These effects are extremely large, of course, in the case of intensely perturbed potentials, as it happens in many adiabatic curves of diatomic hydrides, and noteworthy, in BeH. As we aim to provide benchmark reference data and a rather complete set of spectroscopic parameters for the bunch of states described here, the following procedure has been chosen. The $G(v)$ values have been calculated for each adiabatic potential. The B_v values have been calculated from $\langle 1/R^2 \rangle$ mean values of the corresponding wave functions. The vibrational ω_e, $\omega_e x_e$, and $\omega_e y_e$ parameters have been then obtained from a least squares fitting of the polynomial in $(v+1/2)$, to the n_{lev} lowest $G(v)$ terms. The B_e and α_e have been obtained from the corresponding n_{lev} values by fitting the conventional first degree expression $B_v=B_e-\alpha_e(v+1/2)$. On the other hand, a nonlinear fitting procedure has been applied to the points of each adiabatic potential to get an optimal extended rydberg (ER) function,[96] in the generalized form first proposed by Murrell and Sorbie (MS).[97] The large number of calculated points allows to fit a high degree polynomial in the MS function that has the form

$$V(x) = -D_e P(x)\exp[-a_1 x] + V_\infty, \tag{1}$$

where

$$P(x) = 1 + \sum_{i=1}^{n_d} a_i x^i, \tag{2}$$

with $x=R-R_e$. The power expansion degree has been taken as $n_d=9$, a value that provides the potential with great flexibility and that has been suggested for other hydrides.[98] Hence, each fitting had (n_d+3) freedom degrees (i.e., V_∞, D_e, R_e, and the a_i coefficients). Assuring a similar fitting quality for all the states was a difficult task. Many attempts were required, in particular, for those states that show perturbations at middle and long distances. In a few cases, the fitting is not good enough and leads to large estimated variance values not smaller than $\sim 10^{-6}$ instead of $10^{-8}-10^{-12}$ that have been commonly obtained for those fittings that behave much better.[89]

Once a set of fitted values is assumed, the inertial rotation constants $B_e=h/(8\pi^2 c\mu R_e^2)$ are obtained from the equilibrium R_e values, and quadratic, cubic, and quartic force constants of $V(x)$ have been used to calculate the α_e, ω_e, and $\omega_e x_e$ parameters by means of the expressions first derived by Dunham.[99,100] The R_e, B_e, α_e, ω_e, and $\omega_e x_e$ values obtained from fitted $V(x)$ potentials are reported under the *MS* label in Sec. III D and will be shown and discussed there. Let us advance here that, for some states difficult to fit, the ω_e and $\omega_e x_e$ parameters, as derived from the *MS* force constants, are inconsistent with those obtained from the $G(v)$ values. In these cases, the last values are preferred and the *MS* ones have not been reported.

E. Preliminary study of the GS

The choice of the basis set is of particular importance in the case of a FCI calculation. For the selected hamiltonian, and as far as the Born–Oppenheimer approximation applies, the main source of error comes from the limitations inherent to the basis set. As we want to deal with a single-center augmentation series of diffuse Rydberg ANOs and to follow in detail several excited states along the dissociation coordinate, the basis set must be large enough, but the dimension of the FCI space must be kept into reasonable limits.

In a previous work,[67] the subset $4s2p1d/2s1p$(Be/H) $+4s4p3d$(Be) of the ANO1+Rydberg basis set described in Sec. II A, was used for the FCI calculation of VEE of a large number of excited states of BeH and the results were found reliable.[67] The present work deals with fewer states and the basis set can be slightly larger, hence, the ANO1$+4s4p2d$ previously described in Sec. II A has been used. However, two important points can be raised at this point.

First, the ANO1+Rydberg basis sets lead to short R_e values. Notwithstanding, we decided to go further with this basis set, but a preliminary study comparing to other basis sets has been performed, as shown below.

Second, the $4s4p2d$ (Be) Rydberg augmentation has been kept as centered on Be at all internuclear distances. Several choices for centering these Rydberg AO can be envisaged for distances close to equilibrium, e.g., the centroid

TABLE II. Equilibrium distances, dissociation energies, and some spectroscopic parameters of the $X\,^2\Sigma^+$ state (GS) of BeH.

Basis set[a]	R_e (Å)	D_e (eV)	ω_e (cm^{-1})	$\omega_e x_e$ (cm^{-1})	B_e	α_e	nlev	Dim FCI[b]
ANO1+4*s*4*p*2*d*	1.316	2.245	2125.33	43.0914	10.7300	0.372	6	33357248
ANO1	1.327	2.187	2056.26	39.512	10.3904	0.251	6	3150280
ANO2	1.312	2.355	2213.23	49.15	10.7970	0.361	6	30872736
ANO3	1.322	2.384	2268.62	51.465	10.7318	0.342	6	53877080
Sadlej[c]	1.355	2.066	2048.60	41.256	10.1576	0.334	6	735612
cc-pVTZ[d]	1.339	2.162	2060.25	39.87	10.3898	0.328	6	3150280
cc-pCVTZ[d]	1.345	2.133	2055.52	39.275	10.3055	0.323	6	11766612
Exp[e]	1.3426	2.181	2060.78	36.31	10.3164	0.3030		

[a]ANO1 stands for 4*s*3*p*2*d*1*f*/3*s*2*p*1*d*, ANO2 for 5*s*4*p*3*d*2*f*/4*s*3*p*2*d*, ANO3 or 6*s*5*p*3*d*2*f*/5*s*4*p*2*d*.
[b]Slater determinants in the A_1 symmetry FCI matrix block.
[c]Sadlej polarized basis set (5*s*3*p*2*d*/3*s*2*p*) (Refs. 78 and 79).
[d]Dunning basis set (Refs. 76 and 77).
[e]Experimental values taken from Ref. 46, except dissociation energy (D_e) taken from Ref. 45.

of charges of the cation, the center of masses, the middle bond point, etc. However, no one of these choices seems practical for large bond distances. It should not seem reliable to place these AO at a different point for each distance and, for some choices, it should be placed somewhere in nobody's land at dissociation limit. We have chosen to keep the Rydberg AOs centered in the Be atom. This is a reasonable choice for all the states under consideration because they dissociate to the ground state of H, and to either the GS or a low excited state of Be. Hence, assuring an appropriate description of excited states at long R values is much more important for Be than for H. An important drawback of this choice comes from the limited representation of the high-lying ion-pair dissociation to Be^+ and H^-.

Some spectroscopic parameters calculated for the GS from the FCI potential resulting from several basis sets are reported in Table II. These basis sets are respectively described as ANO1 (the valence set of the present work), ANO2 [5*s*4*p*3*d*2*f*/4*s*3*p*2*d*(Be/H)], and ANO3 [6*s*5*p*3*d*2*f*/5*s*4*p*2*d*(Be/H)]. The two last are larger valence ANO basis sets, but unfortunately, the corresponding *g* ANO functions[68] are not available for Be. The segmented Dunning's basis sets denoted as correlation consistent polarized valence triple dzeta (cc-pVTZ) and correlation consistent polarized core-valence triple dzeta (cc-pCVTZ) have been also used.[76,77] The dimensions of the FCI spaces of the A1 symmetry are reported in the last column of Table II.

The results in Table II are deceiving for the basis set that we have chosen. No other than the basis set can be blamed in this case for the poor performance. The cc-pVTZ and the ANO1 basis set give the same dimension for the FCI space but the former performs better. On the other hand, the 4*s*4*p*2*d* augmentation of ANO1 leads to significant enlargement of the CI space but to a worsening of the results. However, the data in Table II deserve to be considered thoroughly. The results with the ANO2 valence set [5*s*4*p*3*d*2*f*/4*s*3*p*2*d*(Be/H)], that generates a FCI space of similar dimension than the ANO1+Rydberg, are worse, and those from largest ANO3 basis, are still worse. On the other hand, the pCVTZ basis sets improves the R_e and B_e values in respect to the smaller pVTZ but no one of both basis sets are diffuse enough to deal with the Rydberg excited states and the Rydberg-valence mixings in the adiabatic curves. So, faced to the dilemma of using a basis set such as ANO1 +4*s*4*p*2*d* that, on one hand, worsens the GS properties but, on the other, has proven to be reliable for vertical excitations and has been augmented with Rydberg AOs, we have chosen to go further with it. In doing so, we have considered, besides the quality of the VEE, the fact that the FCI adiabatic potentials are always worth as reference benchmarks for approximate methods and that the BeH adiabatic states and their properties (e.g., dipole moments) are so rich in features along the bond dissociation process that offer many challenges to less exact methods.

III. RESULTS

A. Adiabatic curves

The adiabatic potential energy curves of the six lowest $^2\Sigma^+$ states ($X\,^2\Sigma^+$ GS included), and of the two lowest $^2\Delta$ states are plotted in Fig. 1. The first $^4\Sigma^+$ (beyond 1.7 Å) and the first $^2\Sigma^-$ states are also shown in Fig. 1. The curves for the five lowest $^2\Pi$ states and the first $^4\Pi$ state are shown in Fig. 2.

With the only exception of the lowest Σ^+ and Π states (i.e., GS $X\,^2\Sigma^+$ and $A\,^2\Pi$), the states are labeled according to the order numbering of the adiabatic curves as they appear at each symmetry. This is a convenient choice due to the numerous state-state interactions. Similarly, the atomic labeling, e.g., $3s, 3p, 3d, \ldots$, is used for the molecular states as a simplification, usually referred to the dominant character at R_e.

It is apparent from Figs. 1 and 2 that, for most states, the energies beyond $R=5.5$ Å correspond, into $10^{-4}-10^{-5}$ a.u., to those of the separated atoms in their appropriate states. Two noticeable exceptions are the $4\,^2\Sigma^+$ and the $5\,^2\Sigma^+$ states. The potential curves in Figs. 1 and 2 are plotted until $R=8$ Å but the convergence of each state to the energies of the separated atoms is discussed in the next section.

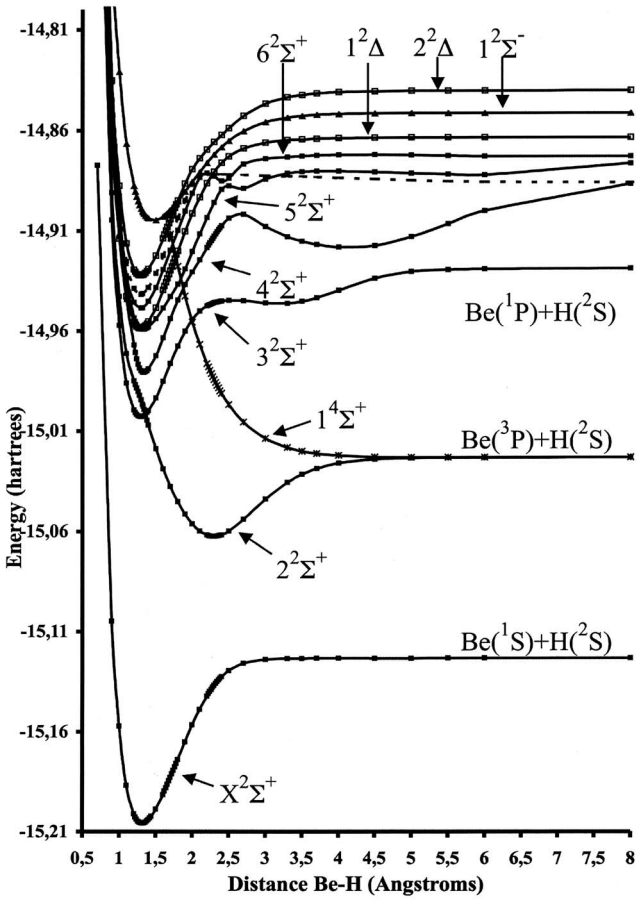

FIG. 1. Adiabatic potential energy curves for the $X\,^2\Sigma^+$ ground state and some of the $^2\Sigma^+$ and $^2\Delta$ excited states as a function of the internuclear distance (in angstroms) for BeH. Dotted lines represent states that do not belong to the converged set at all distances. The lowest atomic dissociation channels are shown on the right.

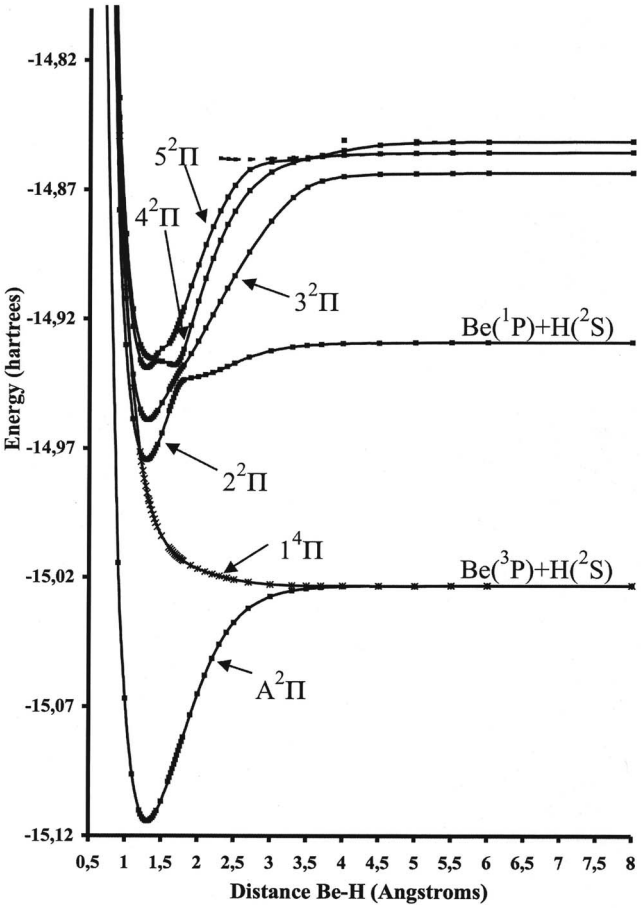

FIG. 2. Adiabatic potential energy curves for some of the $^2\Pi$ excited states as a function of the internuclear distance (in angstroms) for BeH. Dotted lines represent states that do not belong to the converged set at all distances. The lowest atomic dissociation channels are shown on the right.

B. Atomic asymptotes

The atomic states at the dissociation limits must accord to the Wigner–Witmer rules.[101] The GS must correlate with the closed-shell atom of Be and the H doublet $[\mathrm{Be}(1s^2 2s^2;{}^1S)+\mathrm{H}(1s;{}^2S)]$, whereas the next four states ($2\,^2\Sigma^+$, $1\,^4\Sigma^+$, $A\,^2\Pi$, and $1\,^4\Pi$) dissociate into $\mathrm{Be}(1s^2 2s 2p;{}^3P)+\mathrm{H}(1s;{}^2S)$. The first excited state of H, $2s^1$, is at 3/8 a.u. above the GS, so that all the curves here discussed dissociate to $\mathrm{H}(1s;{}^2S)$. As regards the Π doublets, the $2\,^2\Pi$ $(3p)$ dissociates into $\mathrm{Be}(1s^2 2s 2p;{}^1P)$, while $3\,^2\Pi(3d)$, $4\,^2\Pi(4p)$, and $5\,^2\Pi(4d)$ correlate to $\mathrm{Be}(1s^2 2p^2;{}^1D)$, $\mathrm{Be}(1s^2 2s 3p;{}^3P)$, and $\mathrm{Be}(1s^2 2s 3p;{}^1P)$, respectively. The corresponding $^2\Sigma^+$ states can also be related to the same dissociation limits, but the nature of these states changes very often along the adiabatic curves due to numerous avoiding crossings. As an example, the state labeled as $3\,^2\Sigma^+(3s)$ converges to the same limit than the $2\,^2\Pi(3p)$ state.

FCI calculation on the Be atom (i.e., up to quadruples) and on H (CI of singles) with the same basis set $(4s3p2d1f+4s4p2d$ for beryllium, $3s2p1d$ for hydrogen) have been done. The excitation energies of the Be atom are compared in Table III with the experimental terms and with the excitation energies obtained at $R=8$ Å as well. The mean absolute error for the Be states is 0.012 eV and the largest absolute error amounts to 0.019 eV. These values give us an idea about the performance of the basis set used. The FCI energies of Be are given with all the converged figures in column one of Table III.

The FCI roots have size-extensivity and separability properties. Hence, the differences between the excitation values at $R=8$ Å and the Be atom inform us about the achievement of asymptotic behavior at this distance. As mentioned above, the less converged states at this distance are the $4\,^2\Sigma^+$ and $5\,^2\Sigma^+$ states. Notwithstanding, avoided crossings at larger distances must be expected in other states because we get the FCI dissociation limit to the ion-pair $\mathrm{Be}^+(1s^2 2s;{}^2S)+\mathrm{H}^-(1s^2;{}^1S)$ at −14.807 518 07 a.u. [8.5886 eV above $\mathrm{Be}(^1S)+\mathrm{H}(^2S)$], from an independent calculation of the $\mathrm{Be}^+(^2S)$ and $\mathrm{H}^-(^1S)$ fragments with the same basis set, that is expected to be poor for the hydride.

A few additional calculations will serve to get a better estimation of the error in the dissociation limit of the ion-pair $\mathrm{Be}^+-\mathrm{H}^-$, and to know how much this error results from the electron affinity (EA) calculation of H. The experimental dissociation limit (DL), as it results from the experimental values of the ionization potential (IP) of Be (9.322 63 eV) (Ref. 102) and the EA of H (−0.75419 eV),[103] is compared in Table IV to some theoretical values obtained with different basis sets for Be and H. The experimental DL amounts to

TABLE III. Correlation diagrams for low-lying electronic states of BeH.

Be atom[a]				BeH at 8 Å	
FCI energies of the states of Be[b,c]	FCI term of Be[c,d]	Experimental term of Be[d,e]	Dissociation channel (H($1s;^2S$) in all cases)	Excitation Energy[c,d]	States[f]
−14.623 198 643 8	0.0000	0.0000	Be($1s^22s^2;^1S$)	0.000	$X\ ^2\Sigma^+$
−14.523 218 807	2.7206	2.725	Be($1s^22s2p;^3P$)	2.721	$2\ ^2\Sigma^+, 1\ ^4\Sigma^+, A\ ^2\Pi, 1\ ^4\Pi$
−14.428 814 422	5.2894	5.278	Be($1s^22s2p;^1P$)	5.289	$2\ ^2\Pi, 3\ ^2\Sigma^+$
−14.386 021 231 5	6.4539	6.457	Be($1s^22s3s,^3S$)	6.454[g]	$4\ ^2\Sigma^+, 2\ ^4\Sigma^+$
−14.374 415 928 6	6.7697	6.779	Be($1s^22s3s,^1S$)	6.714	$5\ ^2\Sigma^+$
−14.363 398 948	7.0695	7.053	Be($1s^22p^2,^1D$)	7.069	$3\ ^2\Pi, 1\ ^2\Delta, 6\ ^2\Sigma^+$
−14.355 490 374	7.2847	7.289	Be($1s^22s3p,^3P$)	7.284	$4\ ^2\Pi, 2\ ^4\Pi, (7\ ^2\Sigma^+, 3\ ^4\Sigma^+)$
−14.351 250 2	7.4000	7.401	Be($1s^22p^2,^3P$)	7.400	$5\ ^2\Pi, 3\ ^4\Pi, 1\ ^2\Sigma^-, 1\ ^4\Sigma^-$
−14.349 481 218	7.4482	7.462	Be($1s^22s3p,^1P$)	…	$(6\ ^2\Pi, 8\ ^2\Sigma^+)$
−14.340 176 144	7.7014	7.694	Be($1s^22s3d,^3D$)	7.701	$2\ ^2\Delta, 1\ ^4\Delta, (7\ ^2\Pi, 4\ ^4\Pi, 9\ ^2\Sigma^+, 4\ ^4\Sigma^+)$
−14.328 983 384	8.0059	7.988	Be($1s^22s3d,^1D$)		$(^2\Pi, ^2\Delta, ^2\Sigma^+)$
−14.329 787 038	7.9841	7.997	Be($1s^22s4s,^3S$)		$(^2\Sigma^+, ^4\Sigma^+)$
−14.326 524 35	8.0729	8.089	Be($1s^22s4s,^1S$)		$(^2\Sigma^+)$
−14.319 493 888	8.2642	8.283	Be($1s^22s4p,^3P$)		$(^2\Pi, ^4\Pi, ^2\Sigma^+, ^4\Sigma^+)$
−14.318 460 540 8	8.2923	8.311	Be($1s^22s4p,^1P$)		$(^2\Pi, ^2\Sigma^+)$
−14.313 383 1	8.4305	8.423	Be($1s^22s4d,^3D$)		$(^2\Delta, ^4\Delta, ^2\Pi, ^4\Pi, ^2\Sigma^+, ^4\Sigma^+)$

[a]The Be atom calculated with the $4s3p2d1f+4s4p2d$ basis set. The energy of the H atom with the $3s2p1d$ ANO basis set is −0.499 943 934 1 hartrees.
[b]All absolute energies given in hartrees. The decimal places correspond to the convergence reathed for each state. The correlated Be states are given in the fourth column.
[c]This work.
[d]All values in eV. The energies of the terms of the Be atom are relative to the $1s^22s^2\ ^1S$ ground term. The excitation energies correspond to the adiabatic potential curves of BeH and are relative to the energy of the GS $X\ ^2\Sigma^+$ at $R=8$ Å.
[e]Ref. 46.
[f]Corresponding adiabatic states associated to the dissociation channels according to the Wigner–Witmer rules. The states given in parentheses have not been calculated in the present work.
[g]The energy value corresponds to the $2\ ^4\Sigma^+$ states. At this distance the energy value for the $4\ ^2\Sigma^+$ state is lower (6.437 eV). See text for comments.

8.56844 eV but the FCI calculation with the ANO1 $+4s4p2d$ it by 0.02 eV. In order to allow a large and very diffuse basis set for H and its anion, we have used the quadruple augmented cc-pV5Z basis set.[76,104] A CISD calculation (i.e. FCI) reduces the error in the EA to +0.0024 (see Table IV), ten times lower than the error in Beryllium IP. This error is reduced to −0.011 eV if the largest available ANO's valence basis set augmented with the $4s4p2d$ Rydberg set is used in the FCI of Be/Be^+ and the DL is then overestimated by 0.0084 eV (see Table IV).

TABLE IV. Errors in the ionization potential (IP) of Be, electron affinity (EA) of H and dissociation limit (DL) energy of the ion pair Be^+-H^- relative to experimental values. All values given in eV.

Basis set				
Be[a]	H[b]	Δ(IP)[c]	Δ(EA)[d]	Δ(DL)[e]
ANO1−X	ANO1	−0.026 97	+0.047 12	−0.020 14
ANO1−X	q-aug-cc-pV5Z	−0.026 97	+0.002 49	+0.024 48
L−ANO−X	q-aug-cc-pV5Z	−0.010 88	+0.002 49	+0.008 39

[a]ANO1+X stands for ANO1 basis set for Be+$4s4p2d$ Rydberg set. More details in the text. L-ANO−X stands for $7s7p4d3f+4s4p2d$.
[b]ANO1 stands for the ANOI basis set used for H. See text for more details. q-aug-cc-pV5Z stands for quadruple augmented functions for the cc-pV5Z Dunning basis set.
[c]$\Delta(\mathrm{IP})=[E(\mathrm{Be}^+)-E(\mathrm{Be})]-\mathrm{IP}_{\mathrm{exp}}$.
[d]$\Delta(\mathrm{EA})=[E(\mathrm{H}^-)-E(\mathrm{H})]-\mathrm{EA}_{\mathrm{exp}}$.
[e]$\Delta(\mathrm{DL})=(\mathrm{IP}+\mathrm{EA})-(\mathrm{IP}_{\mathrm{exp}}+\mathrm{EA}_{\mathrm{exp}})$. Experimental values: $\mathrm{IP}_{\mathrm{exp}}(\mathrm{Be})=9.322\ 63$ eV (Ref. 102); $\mathrm{EA}_{\mathrm{exp}}(\mathrm{H})=-0.754\ 19$ eV (Ref. 103).

C. Analysis of the nature of the states and avoided crossings

The relatively small $2s$-$2p$ gap of Be atoms results in the relevance of the $(2\sigma)^{-1}\rightarrow(3\sigma)^{+1}$ [HOMO-1 → SOMO] excitation for the lower states of BeH and how this relevance changes with R. This point deserves to be analyzed in more detail, and to be set in relation to the large number of avoided crossings that become apparent in Figs. 1 and 2.

1. $^2\Sigma^+$ states

In the case of the GS, the dominant configuration $(1\sigma^22\sigma^23\sigma^1)$ has a weight (square coefficient) for the most part higher than 0.90 that reaches its maximum value of 0.931 near the equilibrium distance ($R=1.32$ Å). The weight of this configuration and that of the $(2\sigma)^{-1}\rightarrow(3\sigma)^{+1}$ excitation ($1\sigma^22\sigma^13\sigma^2$ occupation) are plotted as a function of the distance, for the GS, in the inset of Fig. 3. The weight of the main configuration dips between 2.0 and 4.5 Å reaching a minimum value of 0.740 at ~3.0 Å due to the raising of some multiconfigurational character as the weight of the [HOMO-1 → SOMO] excitation reaches its maximum value close to 0.095 at ~3.0 Å.

This behavior is relevant in the context of some discussions raised in the past concerning the occurrence of a maximum in the GS potential. Several authors have argued the existence of a potential barrier[37] of at most 200 cm^{-1} that should arise from an avoided crossing with the $C\ ^2\Sigma^+$ va-

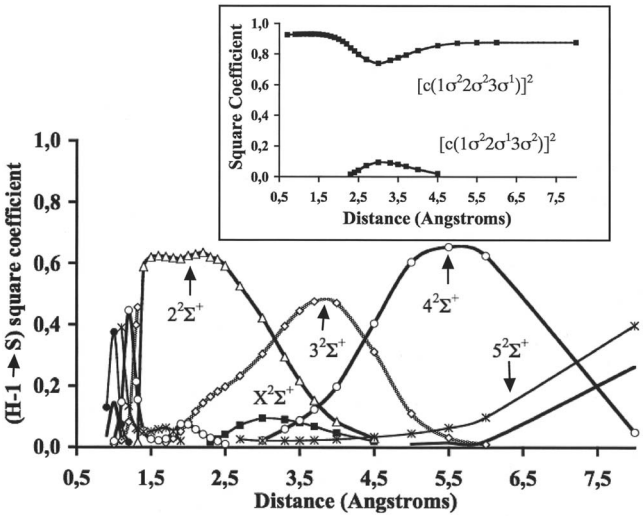

FIG. 3. Squared coefficient of the $(2\sigma)^{-1} \rightarrow (3\sigma)^{+1}$ excitation ($1\sigma^2 2\sigma^1 3\sigma^2$ occupation) in the different $^2\Sigma^+$ states along R. Inset: the squared coefficient of the dominant configuration ($1\sigma^2 2\sigma^2 3\sigma^1$) and that of $1\sigma^2 2\sigma^1 3\sigma^2$ for the GS ($X\ ^2\Sigma^+$) state.

lence state (the $2\ ^2\Sigma^+$ state in Fig. 1, whose nature is discussed below). The present calculation shows no maximum through the curve of the GS (Fig. 1), but the analysis of the FCI wave function places the offset of the $(2\sigma)^{-1} \rightarrow (3\sigma)^{+1}$ contribution in the proximity of 2.3 Å, which, furthermore, is a value close to the equilibrium distance of the $C\ ^2\Sigma^+$ state. Cooper discussed several years ago[50] how the selection of the basis set and the inclusion of the core-valence correlation can modify the shape of the GS potential curve. The present FCI calculations should cover all these aspects, namely, basis set large enough and core-valence correlation.

As concerns the wave function composition, the situation for the $^2\Sigma^+$ excited states is more involved than that of the GS. At the GS equilibrium distance, the $2-6\ ^2\Sigma^+$ states can be classified as the valence $C\ ^2\Sigma^+$ state and the ($3s$, $3p$, $3d$, and $4s$) $^2\Sigma^+$ Rydberg states, respectively (see Fig. 1). However, things become unclear as R changes. Even if one considers only distances larger than the GS R_e, a number of avoided crossings are easily apparent in Fig. 1. An avoided crossing between the 2 and $3\ ^2\Sigma^+$ states occurs at a distance shortly larger than R_e; additional calculations from 1.2 to 1.4 Å with steps of 0.02 Å have helped to place this avoided crossing at 1.36 Å. At about 1.8–1.9 Å, the 4 and $5\ ^2\Sigma^+$ states perturb one another while the nonbonding potential of the $1\ ^4\Sigma^+$ state crosses just there. Another avoided crossing is apparent between the 5 and $6\ ^2\Sigma^+$ states at medium-range distances (~2.4–2.5 Å). The states 3 and $4\ ^2\Sigma^+$ interact at medium- and large-range region (distances larger than 2.7 Å). In this last case, the gap in the perturbation area is rather large and the avoided crossing leads to a broad minimum in the $4\ ^2\Sigma^+$ state at around 4.169 Å that will be the subject of particular attention in Sec. III F.

The analysis of the FCI wave functions along the adiabatic curves reveals the changes in their nature and the complexity associated to these avoided crossings. At very short distances (0.7–1 Å), the states 2, 3, and $4\ ^2\Sigma^+$ can be described as due to s, p, and d Rydberg contributions perturbed by some contribution of the most diffuse components of the H basis set. The $5\ ^2\Sigma^+$ state, instead, is neatly s. It is worthwhile to follow the weight of the $(2\sigma)^{-1} \rightarrow (3\sigma)^{+1}$ excitation in the $^2\Sigma^+$ states at distances larger than 1 Å, (see Fig. 3). In the range from 1 to 1.4 Å, the weight of this configuration jumps from one state to another several times, so revealing the occurrence of several avoided crossings in the shorter-than-R_e region. It dominates the seventh $^2\Sigma^+$ state at 1 Å, the $5\ ^2\Sigma^+$ at 1.1 Å, the $4\ ^2\Sigma^+$ at 1.2 Å, and the $3\ ^2\Sigma^+$ state at 1.3 Å. From 1.4 to ~3 Å, it becomes the leading contribution for the C-$2\ ^2\Sigma^+$ state that has its equilibrium distance in this region (2.30 Å, to be compared with 1.32 Å for the GS). The same excitation dominates again the $3\ ^2\Sigma^+$ curve from ~3.2 to 4.4 Å and the $4\ ^2\Sigma^+$ curve from ~4.5 to 7 Å, where it takes its leading role in the $5\ ^2\Sigma^+$ and so on. A full understanding of these descriptions requires being aware of the changes in the nature of the 2σ and 3σ MOs as R changes. In absence of a symmetry center, the convergence, at long distances, of the one-particle step (ROHF) favors a localized description of the σ and σ^* MOs. At short distances, let us say up to 3 Å, both MOs can be described as resulting from the bonding and nonbonding ($2s_{\mathrm{Be}}$-$2p_{\mathrm{Be}}$) hybrid+($1s_{\mathrm{H}}$). However, as R approaches dissociation, the bonding orbital 2σ becomes a pure $2s$ orbital on Be and the nonbonding 3σ becomes the $1s_{\mathrm{H}}$ orbital. Hence, one can say that the $(2\sigma)^{-1} \rightarrow (3\sigma)^{+1}$ excitation is describing a charge-transfer ion-pair situation (Be^+H^-) at distances larger than 3 Å, because one electron is being promoted from the (mainly $2s_{\mathrm{Be}}$) 2σ MO to the (mainly $1s_{\mathrm{H}}$) 3σ MO. Figures 1 and 3 help us to see that the $(2\sigma)^{-1} \rightarrow (3\sigma)^{+1}$ excitation describes a covalent situation in the region at which it dominates the $2\ ^2\Sigma^+$ state, but describes the (Be^+H^-) ion-pair formation in the regions at which it dominates the $3\ ^2\Sigma^+$ and $4\ ^2\Sigma^+$ states, which is also the region where these states perturb each other.

In summary, concerning the C-$2\ ^2\Sigma^+$ state, the present calculation describe it as dominated by mixed Rydberg s, p, and d contributions at short distances; its valence character increases, promoted by the $(2\sigma)^{-1} \rightarrow (3\sigma)^{+1}$ excitation, at medium-range region (1.4–3 Å) and has again mixed valence and Rydberg character at large distances. Similar descriptions at the appropriate distance ranges can be applied to the $3\ ^2\Sigma^+$ and $4\ ^2\Sigma^+$ adiabatic curves with the help of Fig. 3, and the change in nature of the $(2\sigma)^{-1} \rightarrow (3\sigma)^{+1}$ excitation. This description is in agreement with the analyses reported by different authors[37,41,47,48,53,63,64] concluding that the Rydberg states are perturbed at short distances by the $C\ ^2\Sigma^+$ state to an extent that depends on each particular state and, at large R values, each Rydberg state interacts with the ion-pair $Be^+H^-\ ^2\Sigma^+$ state.[47,48,53]

Other properties, e.g., the $\langle r^2 \rangle$ values, can be of great help in the description of the sates. As an example, if one considers R values slightly larger than the GS equilibrium distance, the $3\ ^2\Sigma^+$ and $4\ ^2\Sigma^+$ states should be classified as the $3s$ and $3p$ Rydberg states, respectively. Notwithstanding, at the GS equilibrium distance itself, the $3s$ Rydberg state, i.e., the $2\ ^2\Sigma^+$, comes first with a VEE of 44 545.76 cm^{-1} (5.523 eV), while the second excited state (i.e., the $3\ ^2\Sigma^+$), with a VEE of about 45 860.43 cm^{-1} (5.686 eV), has more

valence character and should be assigned to the C state. These assignments are assessed by the $\langle r^2 \rangle$ values for these states at the GS R_e, which amounts to 46.00 and 24.85 a.u., respectively (the $\langle r^2 \rangle$ value for the GS itself is 15.20 a.u.). This behavior, of course, is a consequence of the avoided crossing between the 2 and 3 $^2\Sigma^+$ states at the distances near the GS equilibrium distance.

The 5 $^2\Sigma^+$ state can be described as the $(3d)$ $^2\Sigma^+$ Rydberg state. It suffers an avoided crossing at about 2.4–2.5 Å with a higher state (labeled as 6 $^2\Sigma^+$ in Fig. 1) that can be described as having s Rydberg character at short distances and that should correspond to the $(4s)$ $^2\Sigma^+$ state. It must be noted, however, that the adiabatic 6 $^2\Sigma^+$ curve shows a hump at 2.2 Å, that could indicate another avoided crossing with some high-lying curve, not shown in Fig. 1. There is no evidence in our results that the ion pair is present in this region, and the calculated dipole moments that are discussed below, in Sec. III E, are close to zero for these states in this interval of distances.

2. $^2\Pi$

The lowest $^2\Pi$ state corresponds to the well studied A $^2\Pi$ state.[26,39,49,52–54,105–108] Its wave function reveals its mixed valence-Rydberg character due to the single excitation from the 3σ MO to a π virtual MO that mixes Rydberg p functions with valence functions centered in the Be atom. The valence character is dominant for this state, anyway. At large distances, the electron promotion comes from the 2σ MO, which is mainly composed there by the $2s_{\mathrm{Be}}$ AO, allowing the state to dissociate into $\mathrm{Be}(1s^2 2s 2p;{}^3P)+\mathrm{H}(1s;{}^2S)$.

The 2 $^2\Pi$ state is involved, at R values of 1.7–1.8 Å, in a strong interaction with at least two other states, which results into an important perturbation in the adiabatic curve that does not leads to the occurrence of a second minimum in the curve, anyway (see Fig. 2). The double minimum shown by the adiabatic curve of the 4 $^2\Pi$ state is relevant in this context. The potential of the 5 $^2\Pi$ state (the highest Π state calculated) also appears as slightly distorted around 1.4–1.5 Å and shows another avoided crossing at ~3.3 Å, probably associated to the interaction with a higher excited $^2\Pi$ state. This case is similar to that described above for the 6 $^2\Sigma^+$ state.

The analysis of the wave functions for the $^2\Pi$ states is consistent with the complex interaction among them. Some additional points calculated in the region from 1.2 to 2.0 Å help us to locate the first avoided crossing between the 4 and 5 $^2\Pi$ states at 1.42 Å, the second avoided crossing (that seems to involve the 2, 3, and 4 $^2\Pi$ states) in the region of 1.68–1.78 Å, and the abrupt change in the shape of the potential energy curve of the 2 $^2\Pi$ state at ~1.72 Å. At shorter-than-GS R_e distances (1.32 Å), the states are led by excitations from the 3σ MO to π Rydberg virtuals which are πp in the case of the 2 and 4 $^2\Pi$ states and πd in the case of the 3 and 5 $^2\Pi$ states. In the 1.4–1.5 Å range, the 4 and 5 $^2\Pi$ states interchange their p and d dominant character, quite in the region where the 4 $^2\Pi$ state presents the double minimum and the 5 $^2\Pi$ state shows a distinct distortion. Above 1.5 Å and up to a medium-range region (~3.3 Å) the 5 $^2\Pi$ state keeps the πd Rydberg dominant character, and requires excitations from both the 2σ and 3σ MOs. In general, the wave functions of the 2–4 $^2\Pi$ states mix excitations from the 2σ and 3σ MOs to MOs of p and d characters as the bond is stretched. Notwithstanding, the more relevant change in the nature of the wave function occurs in the 3 $^2\Pi$ state that has a great mixing between the p and d Rydberg contributions above 1.8 Å, while in the 2 and 4 $^2\Pi$ states the contribution of the d Rydberg character is smaller. However, at first glance, the adiabatic curves of the 2 and 4 $^2\Pi$ states are those that appear as more perturbed in Fig. 2.

These complex interactions among the $^2\Pi$ states have been described by Machado *et al.*[52] It seems clear that the first avoided crossing (at 1.4 Å) involves only the 4 and 5 $^2\Pi$ states. These authors[52] attribute the second avoided crossing (at 1.7 Å) to an interaction between the 3 and 4 $^2\Pi$ states leading to the second minimum of the latter. The influence of the 2 $^2\Pi$ state in this second minimum cannot be excluded because of the small gap energy among the three states; the smallest gaps in the 1.7–1.8 Å interval are found at 1.74 Å with the following values: $\Delta E(2\,{}^2\Pi\text{-}3\,{}^2\Pi)=0.005\,111$ a.u. (0.139 eV) and $\Delta E(2\,{}^2\Pi\text{-}4\,{}^2\Pi)=0.009\,148$ a.u. (0.249 eV). The 5 $^2\Pi$ curve is also somehow affected. The extent of the participation of the different states in this multistate avoided crossing can be best appreciated from the properties associated to the wave functions, and the dipole moments are of great help for this; the discussion is reported in Sec. III E below. The location of the avoided crossings and the two minima of the adiabatic 4 $^2\Pi$ curve are in good concordance with those reported by Machado *et al.*[52] Also, in agreement with these authors, we find that the 2 $^2\Pi$ potential does not hold a second minimum.

3. $^2\Delta$, $^2\Sigma^-$

The lowest $(3d,4d)$ $^2\Delta$ states (see Fig. 1) are not perturbed by the other calculated states. Both $^2\Delta$ states maintain their d Rydberg character through the whole potential energy curve. These higher-energy states are easily get in the calculation under the A_2 symmetry of the abelian C_{2v} group but the limited size of the Rydberg basis functions $(4s4p2d)$ prevent us from obtaining additional Rydberg Δ states.

The lowest diexcited $^2\Sigma^-$ state crosses under the 2 $^2\Delta$ at ~1.8 Å. This $^2\Sigma^-$ state is composed of diexcitations that promote both 2σ and 3σ electrons to π MOs, and should correspond to the state described by Chan and Davidson[109] as $^2\Sigma^-$ $(1\sigma^2 1\pi^* 2\sigma 1\pi)$. The valence character of the 1 $^2\Sigma^-$ state is assessed by its $\langle r^2 \rangle$ value of 16.14 a.u.

D. Spectroscopic Parameters

Most of the spectroscopic knowledge of BeH is due to the work by Colin and co-workers.[34–37,40,41] In contrast to the detailed knowledge available for the ground and two low states, the experimental data, compiled for other states in common data bases,[46,110] is limited indeed. We intend to learn more about the excited states but having in mind that all the calculated data here reported have been obtained from adiabatic curves.

TABLE V. Equilibrium distances (R_e), dissociation energies (D_e) and some spectroscopic parameters of the calculated states of BeH. (Experimental values in parentheses taken from Ref. 46. Theoretical values used as reference are shown in brackets when experimental values have not been found).

State[a]	R_e (Å)	R_e (Å)-MS[b]	D_e (eV)	B_e	B_e-MS[b]	α_e	α_e-MS[b]	nlev[c]
$X\,^2\Sigma^+$(GS) [X]	1.316 (1.3426)	1.317	2.245 (2.181[d])	10.7300 (10.3164)	10.7264	0.372 (0.303)	0.3435	6
$A\,^2\Pi$(val) [A]	1.309 (1.3336)	1.309	2.479 (2.404[d])	10.8473 (10.4567)	10.8550	0.390 (0.3222)	0.4086	6
$2\,^2\Sigma^+$ [C]	2.293 (2.301[e])	2.293	1.064 (1.048[d])	3.5885 (3.5141[e])	3.5382	0.411 [0.039[f], −0.044[g]]	−0.0011	6
$3\,^2\Sigma^+(3s)$	1.36[h] [1.388[i]]		1.964					
$4\,^2\Sigma^+(3p)$	1.34[h] [1.341[i]]		2.575					
$2\,^2\Pi(3p)$ [B]	1.287 (1.3092)	1.289	1.242 [1.172[j], 1.16[g]]	11.3064 (10.8495) [10.791[g]]	11.1863	0.502 (0.1016) [0.180[g]]	−0.0513	3
$5\,^2\Sigma^+(3d)$ [D]	1.327 (1.325[k])	1.321	2.306 [2.14[g]]	10.2615 (10.599[k]) [10.188[g]]	10.6631	0.438 (0.455[k])	0.7030	5
$3\,^2\Pi(3d)$ [D]	1.307 (1.325[k])	1.309	2.601 [2.50[g]]	10.7985 (10.599[k]) [10.478[g]]	10.8555	0.671 (0.455[k]) [0.368[g]]	0.448	5
$1\,^2\Delta(3d)$ [D] ??	1.289 [1.319[i]] (1.326) [E]	1.288	2.592	11.1868 (10.578)	11.2135	0.374	0.4248	6
$6\,^2\Sigma^+(4s)$ [F?]	1.290 (1.326) [F]	1.285	2.32	11.2300 (10.576)	11.2592	0.419	0.4781	6
$7\,^2\Sigma^+(4p)$ [F?]	1.288	1.286	2.348	11.0688	11.2378	0.345	0.4411	6
$4\,^2\Pi(4p)$ [G?]	1.28, 1.66[h] (1.925) [G] [1.314[j], 1.670[i]]		2.268[l] [2.21[g]]	(5.02)		(−0.556)		
$5\,^2\Pi(4d)$	1.38[h] [1.374[i]]		2.288					
$2\,^2\Delta(4d)$	1.290	1.287	2.509	11.2004	11.2236	0.407	0.5578	5
$1\,^2\Sigma^-$(val)	1.477	1.477	1.456	8.5465	8.5224	0.361	0.3520	6

[a]Notation of Colin and De Greef. (Ref. 36) in brackets. The ? indicates that the assignment is discussed in this work. See text for details.
[b]Obtained from the fitting of a Murrell–Sorbie potential (MS). See text for details.
[c]Number of vibrational levels taken for fitting. See text for details.
[d]Experimental Dissociation energies taken from the work by Le Roy *et al.* (Ref. 45).
[e]Experimental values for C $^2\Sigma^+$ taken from the work by Colin and co-workers (Refs. 36, 37, and 41).
[f]Theoretical calculations by Paldus *et al.* with DZ basis set of Dunning and Hay (Ref. 26).
[g]Theoretical calculations by Henriet and Verhaegen (Ref. 47) [CI with simples, doubles and triples, STO basis set $(24\sigma,13\pi,5\delta)$, and augmented Rydberg functions on Be and H atoms].
[h]Minimum of the adiabatic curve. The vibrational levels have not been used. See text for details.
[i]MRD-CI calculations by Petsalakis *et al.* (Refs. 48 and 53). Basis set: H$(4s2p+1s1p)$ and Be$(12s3p1d+4s3p2d)$.
[j]MR-SDCI calculations of Machado *et al.* (Ref. 52) with essentially a cc-pV5Z basis set.
[k]Experimental values taken from Ref. 41. The experimental values correspond to the so-called "*D* complex." See text for comments.
[l]Dissociation energy from the first equilibrium distance of 1.28 Å. The D_e from the second minimum at 1.66 Å is 2.239 eV.

Some states have been reported experimentally and have received specific labels according with the conventional notation. In this section, we follow the notation of Colin and De Greef.[36] The two valence states labeled as $C\,^2\Sigma^+$ and $A\,^2\Pi$ have been extensively studied[26,28,39,45,49,50,52,54,105–107] and their respective emission bands were reported several years ago.[37,111–114] The experimental parameters of the $C\,^2\Sigma^+$ state correspond to those calculated for the $2\,^2\Sigma^+$ state because all the avoided crossings in which the $C\,^2\Sigma^+$ state is involved occur in the repulsive branch and above the dissociation limit of the state, so that the bound vibrational-rotational levels are not perturbed and the spectroscopical study, at the approached level of the present work, is not complicated by other electronic states.

The spectroscopic parameters for most of the calculated states are reported in Tables V and VI. Data for some states are lacking because providing spectroscopic parameters from the adiabatic potentials should be completely non-sense in these cases. As the most relevant example, the adiabatic curve for the $3\,^2\Sigma^+(3s)$ state shows a sharp and distorted minimum that is merely due to the occurrence, just there, of the avoided crossing with the adiabatic $2\,^2\Sigma^+$ curve. There is no chance that vibrational levels above this crossing be populated for a time larger than a single vibration and predissociation must be expected along the $C\,^2\Sigma^+$ potential. This is in agreement with the absence of absorption spectra for the $3s$ and $3p\,^2\Sigma^+$ states, commonly associated to the predissociative interaction with this valence state.[36,37,47] The equilibrium distance (R_e) and dissociation energy (D_e) reported in Tables V and VI for this $3\,^2\Sigma^+$ state and that for the $4\,^2\Sigma^+$ state must be simply considered as adiabatic potential parameters, good, e.g., for calculation benchmark purposes, but not true spectroscopic parameters. Similar considerations apply to both the double-well $4\,^2\Pi(4p)$ and the $5\,^2\Pi(4d)$ states.

TABLE VI. Electronic Terms (in cm^{-1}) and vibrational spectroscopic parameters (in cm^{-1}) of the calculated states of BeH. (Experimental values in parentheses, taken from Ref. 46).

State[a]	T_e	ω_e	$\omega_e x_e$	$\omega_e y_e$	nlev[b]	G(0)	ν_{00}	ω_e-*MS*[c]	$\omega_e x_e$-*MS*[c]
$X\ ^2\Sigma^+$(GS) [X]	…	2128.55 (2060.78)	44.924(36.31)	0.2336(−0.38)	6	1054.2	…	2120.39	37.986
$A\ ^2\Pi$(val) [A]	20 055.83 (20 033.19)	2155.5 (2088.58)	47.769(40.14)	−0.0451(−0.47)	6	1064.8	20 066.43 (20045.81)	2158.26	50.676
$2\ ^2\Sigma^+$ [C]	31 461.31	1018.7 [1061.12[d]]	16.491(42.19[d])	−0.8255	6	498.4	30 905.51 (30971.52[d])	1040.09	25.229
$3\ ^2\Sigma^+(3s)$	44 916.77[e]								
$4\ ^2\Sigma^+(3p)$	49 385.06[e] (48 876.93[f])								
$2\ ^2\Pi(3p)$ [B]	50 797.20 (50 882)	2288.6 (2265.94)	34.638(71.52)	−9.2801	3[g]	1134.5	50 877.50 (50976.17)	1998.71[c,*]	−289.78*
$5\ ^2\Sigma^+(3d)$ [D]	54 037.43 (54 158.86[h])	2057.2 (1890.5[h])	103.52(72.8[h])	5.1621	3[g]	1003.4	53 986.63 (54050)	2418.01[c,*]	289.67*
$3\ ^2\Pi(3d)$ [D]	54 155.07 (54 158.86[h])	2072.3 (1890.5[h])	102.79(72.8[h])	−5.5895	3[g]	1009.8	54 110.67 (54050)	2043.74	56.936*
$1\ ^2\Delta(3d)$ [D]	54 209.62 (54 158.86[h])	2288.3 (1890.5[h])	48.190(72.8[h])	0.05796	6	1130.6	54 286.02 (54050)	2317.42	64.37
??	(54 134) [E]	(1970)					(54 097.6)		
$6\ ^2\Sigma^+(4s)$ [F?]	56 253.90 (56 606) [F]	2282.5 (2153)	37.180	−1.4745	3[g]	1131.7	56 331.40 (56661.24) [F]	2933.75[c,*]	428.16*
$7\ ^2\Sigma^+(4p)$ [F?]	57 941.31	2299.0	36.669	−2.4461	5	1138.9	58 026.01	2266.79	23.506
$4\ ^2\Pi(4p)$ [G?]	58 563.60[e,i] (58 711)						(57 886.2)		
$5\ ^2\Pi(4d)$	59 329.82[e] (60 168.63[j])								
$2\ ^2\Delta(4d)$	59 994.08	2273.9	46.138	−1.0503	5	1124.06	60 063.94	2235.68	36.057
$1\ ^2\Sigma^-$(val)	66 047.46	1496.9	24.410	−1.5924	6	736.7	65 729.96	1518.31	32.895

[a]Notation of Colin and De Greef.[36] can be taken from Table V. The ? indicates that the assignment is discussed in this work. See text for details.
[b]Number of vibrational levels taken for fitting. See text for details.
[c]Obtained from the fitting of a Murrell–Sorbie potential (MS). See text for details. The (∗) indicates the cases where the vibrational parameters calculated from a Murrell–Sorbie potential are too much inconsistent with those obtained from the G(v) values.
[d]Experimental values for C $^2\Sigma^+$ taken from the work by Colin and co-workers (Refs. 36 and 41).
[e]Adiabatic excitation energies obtained directly from the adiabatic potential curves. They are obtained as energy difference between the excited state at calculated minimum and the GS at its equilibrium geometry.
[f]Experimental value estimated in Refs. 36 and 63.
[g]Strongly perturbed states at low vibrational levels. See footnote c above.
[h]Experimental values taken from Ref. 41. The experimental values correspond to the so-called "*D* complex". See text for comments.
[i]Adiabatic energy with respect to the first equilibrium distance of 1.28 Å. The T_e, from the second minimum at 1.66 Å is 58789.43 cm^{-1}.
[j]Experimental value taken from Ref. 36 converted to vertical excitation energy.

The R_e, D_e and (B_e, α_e) conventional vibration-rotation coupling parameters are collected in Table V, including those for the two $^2\Delta$ and the $1\ ^2\Sigma^-$ states. The values have been obtained independently in the two ways described in Sec. II D; namely, from the *MS* fit on one hand and from the $G(v)$ levels on the other. The number of vibrational (v) levels used in each case is indicated in the last column of Table V. In order to get a common standard for comparisons, we have selected the first six values, i.e., from B_0 to B_5, except for those states where a serious perturbation in the sequence of vibrational gaps was evident. This was the case for the D-5 $^2\Sigma^+(3d)$, D-3 $^2\Pi(3d)$, and $2\ ^2\Delta(4d)$ states, where five levels have been used, and for the B-2 $^2\Pi(3p)$ state where only three vibrational levels can be considered as relatively unperturbed before the abrupt distortion in the adiabatic curve at 1.7–1.8 Å is reached by the vibrational levels.

The values obtained from the *MS* fit are extremely sensible to small variations of the whole potential as the fit spans all the range of distances. Hence, when significant discrepancies occur between the two sets of R_e, B_e, and α_e values, they can be attributed, in principle, to the difficulties faced by the fitting procedure in order to deal with the perturbed potentials at medium or large-range distances. Notwithstanding, some disagreements occur in curves that do not seem to be perturbed, such as the C-2 $^2\Sigma^+$ state. Two completely inconsistent values of α_e are found, even if the calculated points at $R \leqslant 1.4$ Å are removed from the MS fit. Less surprising are the discrepancies in the (B_e, α_e) values for the B-2 $^2\Pi(3p)$ and D-5 $^2\Sigma^+(3d)$ states, because the fitting of these featured potentials to the MS function was specially difficult.

The experimental values, available for a few states only, have been included in Table V as a reference. In a number of cases, calculated values from other theoretical works have been included with the same purpose. The actual $G(v, J=0)$ levels obtained by solving the one-dimensional Schrödinger equation, as well as the absolute FCI values of the potential energy curves of all the discussed states, are provided in the EPAPS file[115] for convenience of the interested reader.

Consistent with the underestimation of R_e for the GS, the basis set leads to an overestimation of the dissociation energy. The D_e value (2.245 eV), can be compared either with

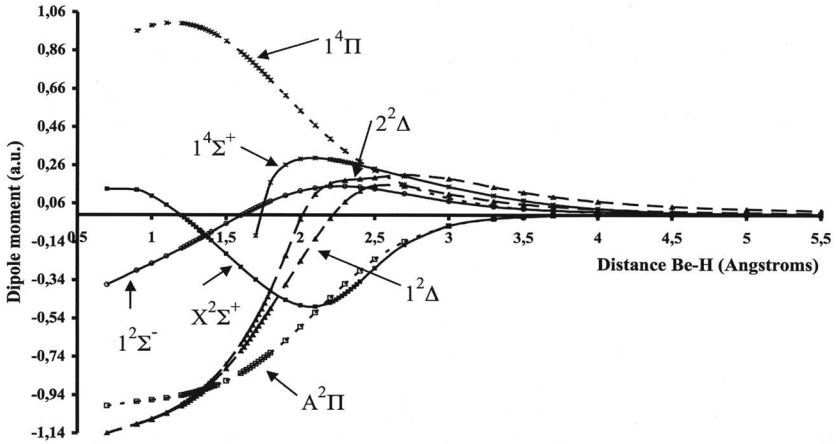

FIG. 4. Dipole moments in a.u. as a function of internuclear distance for the $X\,^2\Sigma^+$, $1\,^4\Sigma^+$, $A\,^2\Pi$, $1\,^4\Pi$, $1\,^2\Delta$, $2\,^2\Delta$, and $1\,^2\Sigma^-$ states.

the most recent experimental value (2.181 ± 0.025 eV) by Le Roy *et al.*[45] or with that of 2.161 ± 0.012 eV reported by Colin and co-workers[37,40] that has been commonly used as a reference in the past. Experimental D_e values[45] for the $A\,^2\Pi$ and $C\,^2\Sigma^+$ states are 2.404 ± 0.025 and 1.048 ± 0.025 eV, respectively. They are also overestimated by the present FCI values (see Table V).

The electronic terms (T_e), zero point energies [$G(0)$], ν_{00} values, and other vibrational parameters are reported in Table VI. The n_{lev} column indicates the number of values of $G(v)$ used in the fitting calculation of the vibrational parameter set ($\omega_e, \omega_e x_e, \omega_e y_e$). Some idea about the reliability of these fitted parameters can be get against the $G(0)$ values that are given in column seven. The arbitrary value of $n_{\text{lev}}=6$ has been used when the mean error in the $G(v)$ residuals could be kept in a range of a few units of cm^{-1} (preferably $1-2\ \text{cm}^{-1}$). When this was not possible, fewer levels were used, as indicated. In these cases, the disagreement between the *MS* parameters and the fitted ones is larger.

In those cases where either T_e or ν_{00} values can be clearly compared with experiment, the present calculations are in small error, showing that for the purpose of vertical calculations the basis set works well. Some relevant discrepancies are present, but they deserve special attention. Let us note that the states associated to the 3*d* Rydberg orbital have been normally treated as a 3*d* complex, giving a group of $\ell\lambda$ substates $D(^2\Sigma^+, ^2\Pi, \text{and } ^2\Delta)$ that form together what has been called the $\ell=2$ Rydberg molecular complex.[41] The so-called "*D* complex" at $54\,000\ \text{cm}^{-1}$ can be effectively resolved in three Rydberg (3*d*) states that are distinctively characterized as $5\,^2\Sigma^+$, $3\,^2\Pi$, and $1\,^2\Delta$. The $\nu_{00}=T_e+G_0'-G_0''$ values for the *D* states show errors lesser than $100\ \text{cm}^{-1}$ relative to the experimental values and appear in the same order than the T_e values.

However, the characterization of some experimentally reported states is unclear and does not agree with the theoretical adiabatic curves. One of these cases is that of the 4*s* and 4*p* Rydberg states of Σ^+ symmetry that are commonly labeled as *E* and $F\,^2\Sigma^+$, respectively.[36] Given the small errors found for the lower states, the results for the $6\,^2\Sigma^+(4s)$ and $7\,^2\Sigma^+(4p)$ states should be disappointing if they were to be assigned to the experimental *E* and *F* states. We have then attempted to assign these states by assuming that there is not calculated evidence of the *E* state. Consequently, the *F* state should correspond to the $6\,^2\Sigma^+(4s)$ state instead of the $7\,^2\Sigma^+(4p)$. It is worth to remember that the labelling of the $E\,^2\Sigma^+$ and $F\,^2\Sigma^+$ states comes from an early work by Colin and De Greef[36] that reported two states with ν_{00} values of about 54 100 and 56 600 cm^{-1}, respectively. The calculated $6\,^2\Sigma^+(4s)$ state lies at an energy ($T_e=56\,253.9\ \text{cm}^{-1}$, $\nu_{00}=56\,331.4\ \text{cm}^{-1}$), that is, fairly higher than that of the $(3d)D$ state, so confirming an earlier theoretical prediction of Henriet and Verhaegen[47] but in disagreement with the assignment by Colin and De Greef. There is no evidence, indeed, in the present calculations, of the presence of any $^2\Sigma^+$ state near 54 100 cm^{-1} other than the $5\,^2\Sigma^+(3d)$ state. The calculations indicate that the $6\,^2\Sigma^+(4s)$ state agrees energetically better with the experimental state found at $\nu_{00}=56\,661.24\ \text{cm}^{-1}$ ($F\,^2\Sigma^+$) and this result corroborates another by Petsalakis *et al.*[53] Then, for the $7\,^2\Sigma^+(4p)$ state, with $\nu_{00}=58\,026.01\ \text{cm}^{-1}$, we have not found experimental counterpart to assign it. It must be noted that Clerbaux and Colin recognized in a subsequent study that their assumption of an $E\,^2\Sigma^+$ state that should lie in near coincidence with the $3\,^2\Pi(3d)$ state could be erroneous.[41] Finally, the adiabatic states $6\,^2\Sigma^+$ and $7\,^2\Sigma^+$ exhibit similar calculated properties, as a consequence of their potentials having a similar shape but appearing as displaced one from the other by $\sim 2400\ \text{cm}^{-1}$ (0.3 eV).

Another controversial case is related to the characterization of an experimental state reported long time ago by Colin and De Greef as $G\,^2\Pi$.[36] These authors assigned large equilibrium distance of $R_e=1.925$ Å and spectroscopic parameters of $\omega_e=405.3\ \text{cm}^{-1}$, $\omega_e x_e=22.7\ \text{cm}^{-1}$ and $\alpha_e=-0.556\ \text{cm}^{-1}$; however, computational evidence for such a minimum has never been found in the low $^2\Pi$ states. Moreover, the occurrence of a double well in the $4\,^2\Pi$ state, with minima at 1.28 and 1.66 Å, does not seem to be compatible with the R_e value of Colin and De Greef.[36] Colin and co-workers[36,37,41] have assumed that the *B* and $G\,^2\Pi$ should arise from an avoided crossing between two $^2\Pi$ states; however, the high level calculations reveal a more complex interaction involving more than two $^2\Pi$ states, as it was discussed in Sec. III C (cf. Sec. III E below). This multistate interaction agrees with previous theoretical studies.[47,52] The T_e value assigned to the $G\,^2\Pi$ state could agree with the

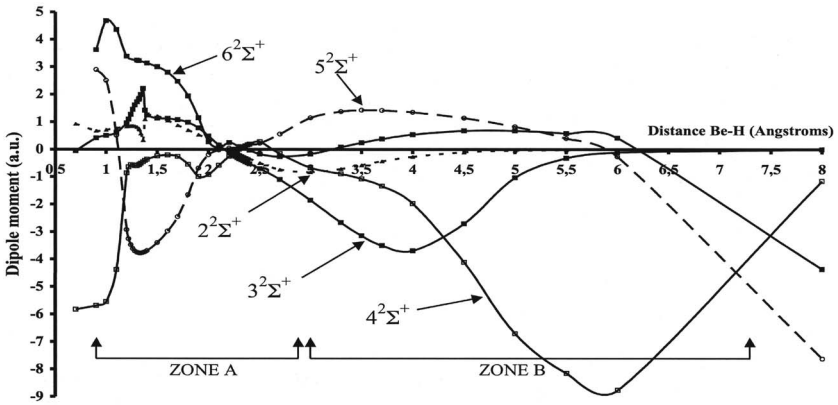

FIG. 5. Dipole moments in a.u. as a function of internuclear distance for the $2-6\ ^2\Sigma^+$ excited states.

calculated adiabatic excitation energies of the $4\ ^2\Pi(4p)$ state shown in Table VI, but, on the basis of the few spectroscopic parameters available, the observed transition assigned to $G\ ^2\Pi$-$X\ ^2\Sigma^+$ does not refer to the theoretical $4\ ^2\Pi(4p)$ state. This problem has been repeatedly pointed out by other authors, such as Henriet and Verhaegen,[47] Petsalakis *et al.*,[53] and Machado *et al.*[52] The experimental data associated to the $B\ ^2\Pi$ and $G\ ^2\Pi$ states should need reinterpretation, as already discussed by Machado *et al.*,[52] and as our calculations should confirm: the transition assigned to the $G\ ^2\Pi$-$X\ ^2\Sigma^+$ band system could be more likely interpreted as coming from the high-lying vibrational levels of the $2\ ^2\Pi(3p)$ state, and the transition associated to the so-called[36] $B'\ ^2\Pi$-$X\ ^2\Sigma^+$ as coming from the $v'>3$ vibrational levels of the same $2\ ^2\Pi(3p)$ state. Four vibrational levels can be calculated for this state ($v'=0-3$) in the FCI adiabatic potential of this work before attaining the strong avoided crossing suffered at about 1.7 Å. Note, however, that this interpretation of the $G\ ^2\Pi$ and $B'\ ^2\Pi$ states would require that vibrational levels at energies higher than the avoided crossing can be reached without leading to immediate predissociation.

Machado *et al.*[52] pointed out the important effect of the basis set in order to obtain a correct description for the high-lying $^2\Pi$ states. These authors reported the two minima for the $4\ ^2\Pi$ state at 1.314 and 1.670 Å (see Table V). We find a barrier between these minima at 565 cm^{-1} from the deepest minimum and it is located at ~1.42 Å, while Machado *et al.*[52] reported a barrier of 645 cm^{-1} and located it at 1.459 Å. Both the CDIST and LEVEL8.0 programs can calculate the vibrational levels for this adiabatic double-well $4\ ^2\Pi$ potential but these levels should be unlikely reachable to measurement as the avoided crossing should predissociate the molecule along the $2\ ^2\Pi(3p)$ curve. Spectroscopic data for the $4\ ^2\Pi$ curve are not reported because these levels do not behave as slightly anarmonic series of vibrational levels.

E. Dipole moments

The calculated dipole moments (DMs) as a function of the internuclear distance along the adiabatic curves are shown in Figs. 4–6. The DMs of five doublet states ($X\ ^2\Sigma^+, A\ ^2\Pi, 1\ ^2\Delta, 2\ ^2\Delta, 1\ ^2\Sigma^-$) and two quadruplet states ($1\ ^4\Sigma^+$, and $1\ ^4\Pi$) are shown in Fig. 4. Those of the excited $^2\Sigma^+$ states are shown in Fig. 5 and those of the $^2\Pi$ states in Fig. 6. Grouped in this way, the different behavior of the DM curves for each group is made apparent. This behavior can be associated with either the occurrence or not of sudden changes due to interactions among the states, and to the dissociation to neutral or charged fragments.

Negative values of the electrical dipole correspond to the dipole arrow pointing toward the Be atom. Be is less electronegative than H, and, accordingly, the dipole moment is found negative for the GS, even though the basis set somehow favors the electronic density on the Be atom.

Several points of DM sign inversion and steep dependencies on R can be found for the states of BeH at short (and medium) distances. These jumps in a given curve imply that for the molecule to follow the adiabatic potential, a strong

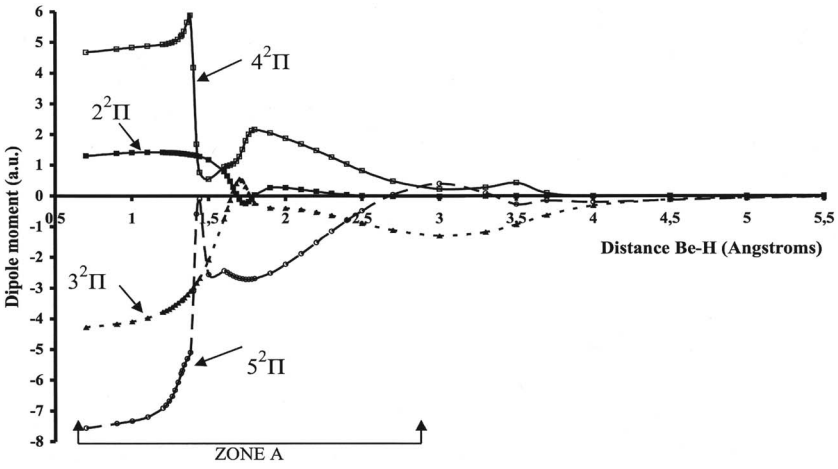

FIG. 6. Dipole moments in a.u. as a function of internuclear distance for the $2-5\ ^2\Pi$ excited states.

change of its electronic structure is required in a short interval of R. Consequently, a breakdown of the Born–Oppenheimer assumption must be expected at these points or at short intervals of distances around them. Such jumps are found in the DM curves of BeH for many states even at typical bond distances.

The states represented in the Fig. 4 display no sharp features as well as a common asymptotical behavior in which the DM trends to zero at larges distances, in accordance with dissociation into neutral atoms (Be and H). All states, except the $A\ ^2\Pi$ state, show singular points (either maxima or minima) in the DM curves. The FCI values and locations of these stationary points are $X\ ^2\Sigma^+$ (−0.477 51 a.u. at R =2.1 Å), $1\ ^2\Delta$ (+0.152 98 a.u. at R=2.5 Å), $2\ ^2\Delta$ (+0.209 33 a.u. at R=2.7 Å), $1\ ^2\Sigma^-$ (+0.150 16 a.u. at R =2.3 Å), $1\ ^4\Sigma^+$ (+0.297 84 a.u. at R=2.1 Å), and $1\ ^4\Pi$ (+1.002 75 a.u. at R=1.1 Å). For the valence state $A\ ^2\Pi$, the DM decreases smoothly from very high negative values at short distances to zero near dissociation.

The small perturbation at $R\sim2.5$ Å in the DM curve of the $2\ ^2\Delta$ state suggests a small interaction that is also apparent in a thorough look at the energy curve.

In contrast to the states reported before, the very featured behavior of the DM along the $^2\Sigma^+$ and $^2\Pi$ adiabatic states (Figs. 5 and 6) deserves attention. Let us consider two zones in the Σ^+ states for convenience: a short-range region (zone A in Fig. 5) and a medium-to-large-range region (zone B in Fig. 5).

At the distance of the avoided crossing between the states 2 and $3\ ^2\Sigma^+$ (1.36 Å), their DM curves change abruptly (see zone A of Fig. 5). In this case, both adiabatic states have similar dipole moments before and after the avoided crossing. The interaction between these two states is maximal at this distance, where the adiabatic curves approach the most one the other.

Figure 5 helps also to locate the avoided crossing region between the $4\ ^2\Sigma^+$ and $5\ ^2\Sigma^+$ states at short distances (1.1–1.2 Å). A hump in the DM curve of the $6\ ^2\Sigma^+$ state occurs just in the same range, so revealing that this state is also involved, but in a more limited way, in the coupling. In a similar way, the DM curves indicate that the avoided crossing between the $4\ ^2\Sigma^+$ and $5\ ^2\Sigma^+$ states at 1.87 Å could involve the $6\ ^2\Sigma^+$ state whose DM changes following a decreasing curve that mirrors the ascending one of the $5\ ^2\Sigma^+$.

Several perturbations seem to affect the $^2\Sigma^+$ states in the neighborhood of 2.2 Å, a region where the DM value is close to zero. These interactions involve also the $6\ ^2\Sigma^+$ adiabatic state that shows an oscillatory behavior in both the energy and the DM curves in the region immediately above 2.0 Å.

The most relevant feature in zone B is the occurrence of large negative dipole moments as a consequence of the development of the charge-transfer ion pair Be^+H^- that jumps from one state to the next one as R increases. The DM of the $2\ ^2\Sigma^+$ state (that corresponds with the experimental $C\ ^2\Sigma^+$ state at long distances) tends quickly to zero in zone B. Meanwhile, the $3\ ^2\Sigma^+$ and $4\ ^2\Sigma^+$ states show high negative values in two consecutive regions: ~3.0–4.5 Å for the $3\ ^2\Sigma^+$ state and ~4.5–7.0 Å for the $4\ ^2\Sigma^+$ state. These two regions correspond, of course, to those at which the interaction with the ion pair (Be^+H^-) occurs, as it was discussed in Sec. III C. Hence, these are the regions at which the $(2\sigma)^{-1}\rightarrow(3\sigma)^{+1}$ excitation has charge-transfer character and dominates the description of these states (see Fig. 3). High DM values, increasingly closer to the values of R in atomic units (as it should correspond to the transfer of a unit charge), occur in each state, and can be expected to be larger and larger. One can imagine the dissociation to the ionic pair as occurring through a succession of ion-pair regions of $^2\Sigma^+$ states as R tends to infinite. Notwithstanding, each one of these $^2\Sigma^+$ states dissociate to neutral Be and H.

TABLE VII. Dipole moments of ground and excited states of BeH at the GS R_e. The oscillator strengths to each excited state are also given.

States	DM (a.u.)	OS
$X\ ^2\Sigma^+$	−0.078 21	
$2\ ^2\Sigma^+$	+0.757 44	0.0525
$3\ ^2\Sigma^+$	+1.814 94	0.0031
$4\ ^2\Sigma^+$	−0.559 68	0.0544
$5\ ^2\Sigma^+$	−3.773 35	0.0962
$6\ ^2\Sigma^+$	+3.219 32	0.0069
$7\ ^2\Sigma^+$	+2.541 96	0.0153
$A\ ^2\Pi$	−0.918 58	0.0926
$1\ ^4\Pi$	+0.979 82	
$2\ ^2\Pi$	+1.386 84	0.0505
$3\ ^2\Pi$	−3.397 25	0.0573
$4\ ^2\Pi$	+5.194 33	0.0379
$5\ ^2\Pi$	−5.779 81	0.0400
$1\ ^2\Delta$	−0.932 80	
$2\ ^2\Delta$	−0.920 80	
$1\ ^2\Sigma^-$	−0.123 74	

The $^2\Pi$ states dissociate to neutral fragments and consistently their DMs, which are plotted in Fig. 6, tend to zero at large distances. The coupling between the adiabatic $4\ ^2\Pi$ and $5\ ^2\Pi$ curves is revealed as a sharp feature in the DM curves at 1.4 Å. In this case, the DMs in both states are large and have opposite sign, so that the curves do not cross. The $2\ ^2\Pi$ and $3\ ^2\Pi$ are not involved in this avoided crossing, but things seem to be a bit more complex in the 1.6–1.8 Å region, where the interaction of the $2\ ^2\Pi$ and $3\ ^2\Pi$ states is clear but the $4\ ^2\Pi$ and $5\ ^2\Pi$ states should be also involved, as suggested by the adiabatic curves in Fig. 2. Finally, the perturbation between the $4\ ^2\Pi$ and $5\ ^2\Pi$ states in the region of 3–4 Å is reflected also by the DM curves.

A list of the DM values at the GS equilibrium distance for all the studied states is reported in Table VII. They compare well to those obtained in a previous work[67] where they were discussed together with some highest states. Few works have been devoted to the study of the electric moment properties of BeH. In particular, Henriet and Verhaegen[47] reported dipole moment values for some states obtained with a large STO basis set and a frozen-core two-step CI procedure that included singles, doubles and triples. The values obtained by these authors at their equilibrium distances for each state were $X\ ^2\Sigma^+$, −0.0944 a.u. (R_e=1.345 Å); $C\ ^2\Sigma^+$, −0.169 17 a.u. (R_e=2.301 Å); and $A\ ^2\Pi$, −0.904 87 a.u. (R_e=1.334 Å). These values agree with those reported here

into 0.01–0.02 a.u. provided that similar distances are considered and after realizing that these authors use the $C\,^2\Sigma^+$ label all along the $2\,^2\Sigma^+$ adiabatic curve. As an example, we obtain for the $C\,^2\Sigma^+$ state a DM value of −0.155 43 a.u. at $R=2.30$ Å, which is to be compared to that of Henriet and Verhaegen given above.

F. The flat well of the $4\,^2\Sigma^+$ state at 4 Å

The avoided crossing between the $3\,^2\Sigma^+(3s)$ and $4\,^2\Sigma^+(3p)$ states in the 4–5 Å region deserves special attention. We can locate the starting distance of this interaction at ~4 Å with the help of Fig. 5 that, at the same time, shows no evidence of other states being involved in this coupling. This two-level avoided crossing results in a large interaction that leads to a flat minimum in the adiabatic curve of the $4\,^2\Sigma^+$ state. One can wonder if this smooth energy well could hold some vibrational levels. With the potential being so flat, small vibrational energies can be expected and, consequently, small vibrational velocities can be assumed. According to the Landau–Zener model,[116,117] slow movement along with large gap should favor the probability that the system will remain in the adiabatic surface, even if a change of electronic structure along the adiabatic curve is required. In the present case this change should involve the developing further and back of the ion-pair charge transfer at each vibration. We calculate the first five vibrational levels that could be hold by the adiabatic well of the $4\,^2\Sigma^+$ state around the minimum at 4.1 Å at $G_v=128.03$, 475.55, 824.87, 1173.06, and 1602.67 cm^{-1} (the probability of tunneling through the hump at 2.5 Å has not been considered). These are low energy vibrations as expected from the potential flatness. The probability of adiabatic behavior in the simpler Landau–Zener model for the tunneling transition between two diabatic states, Ψ_A and Ψ_B,[116,117] can be calculated as

$$P_{\mathrm{ad}} = 1 - P_{LZ} = 1 - \exp(-2\pi\gamma), \tag{3}$$

with

$$\gamma = \frac{H_{AB}^2}{\hbar \cdot \frac{dR}{dt} \cdot \left| \frac{\partial E_A}{\partial R} - \frac{\partial E_B}{\partial R} \right|}, \tag{4}$$

where H_{AB} is the off-diagonal interaction term between Ψ_A and Ψ_B, which is supposed to be linearly dependent with time, and $|\partial E_A/\partial R - \partial E_B/\partial R|$ is the absolute value of slopes difference, at the crossing point, of the diabatic (i.e., crossing) E_A and E_B curves.

Following the procedure of Henriet and Verhaegen,[47] we have approximated H_{AB} by $\Delta E/2$, i.e., half of the gap value at the crossing point; dR/dt can be related to the mean kinetic energy, that is taken on average as the vibrational energy for each level, E_v. So, in atomic units, one can write

$$\gamma = \frac{(\Delta E)^2}{4 \cdot \sqrt{2/\mu} \cdot \Delta s \cdot \sqrt{E_v}}, \tag{5}$$

where the reduced mass is $\mu=1652.36$ a.u. for BeH and Δs stands for the absolute value of the slopes difference. The crossing point for calculating the slopes has been located, according to Fig. 5, in 4.6 Å, so that $\Delta s \sim 0.014\,56$ a.u. and $\Delta E=0.016$ a.u. With these values, the probabilities of the diabatic jump, P_{LZ}, range from 10^{-15} to 6.5×10^{-5}, as one goes from $v=0$ to 5. The model predicts that an essentially adiabatic behavior must be expected in this minimum, so that some chance exists that these vibrational states could be populated, at least the lowest ones. The spectroscopic constants calculated from the first three G_v values given above are $R_e=4.170$ Å, $\omega_e=277.7$ cm^{-1}, $\omega_e x_e=-21.40$ cm^{-1}, $B_e=1.075$ cm^{-1}, and $\alpha_e=-0.023$ cm^{-1}.

G. Transition dipole strengths

This section is focussed on the dipole allowed transitions from the GS ($X\,^2\Sigma^+$). The transition dipole strength (TDS) values have been calculated along the dissociation coordinate as square absolute value of the transition dipole moment, $\langle \mathrm{exc}|\hat{\mu}|0\rangle$. For parallel transitions ($X\,^2\Sigma^+ \rightarrow {}^2\Sigma^+$), this quantity is calculated as $\langle X\,^2\Sigma^+|\hat{\mu}_x|^2\Sigma^+(i)\rangle$ for each $^2\Sigma^+(i)$ excited state. In the case of perpendicular transitions involving the $^2\Pi$ states, in the framework of the C_{2v} abelian subgroup, the Π_y and Π_z components [i.e., $\langle X\,^2\Sigma^+|\hat{\mu}_\alpha|^2\Pi_\alpha(i)\rangle; \alpha=(y,z)$, which transform like the coordinates y and z] have been obtained, rather than the Π_+ and Π_- ones. For $\Pi \leftrightarrow \Sigma$ transitions, the matrix element $\langle \Sigma|\hat{\mu}_\alpha|\Pi_\alpha\rangle; \alpha=(y,z)$ equals[118] to $\langle \Sigma|(\hat{\mu}_y \pm i\hat{\mu}_z)/2^{1/2}|\Pi_\pm\rangle$ and, consequently, the square absolute values are equivalent in both representations.

The TDS curves from the GS to the $^2\Sigma^+$ states and to the $^2\Pi$ states are shown in Figs. 7 and 8, respectively.

It has been suggested that the analysis of the features of the TDSs can be useful for studies of selective excitation pathways and photofragmentation dynamics.[119,120] The TDS for these transitions reveals several pronounced maxima that are located at different distances depending on the excited state. It matters to note that at distances larger than 3 Å, where the GS potential curve has already attained a plateau (see Fig. 1), only a few states [e.g., $3\,^2\Sigma^+$ and $2\,^2\Pi$ that dissociate to $\mathrm{Be}(^1P)+\mathrm{H}(^2S)$] present high TDS values, while for the remaining states the TDS tend to zero. This behavior at the dissociation limit must be related, of course, to the few transitions that are allowed in the closed-shell Be atom. Now, the avoided crossing between the $3\,^2\Sigma^+$ and $4\,^2\Sigma^+$ states in the 3.0 to 5.0 Å region is clearly apparent in the oscillations of TDS curves of these states. This is the region of the second energy well of $4\,^2\Sigma^+$, whose TDS curve reaches its maximum at about 3.7 Å (see Fig. 7). One could wonder if the second well of $4\,^2\Sigma^+$ could be reached through a photoexcitation to a high vibrational level of the $5\,^2\Sigma^+$ that has the greatest TDS at the GS R_e. Even if such a transition were to be allowed by Franck–Condon factors, there is little chance that the second minimum of $4\,^2\Sigma^+$ be reached in this way because predissociation is much likely to occur due to the avoided crossing near 2.0 Å where the $1\,^4\Sigma^+$ state curve crosses those of $5\,^2\Sigma^+$ and $4\,^2\Sigma^+$ states.

It can be noticed also that the large TDS values of the $3\,^2\Sigma^+$ and $4\,^2\Sigma^+$ states are developed in the right branch ($R \geqslant R_e$) of the GS energy curve that corresponds to the beginning of the dissociation steps. It is interesting to note that the TDSs to each state are small in the regions where its leading excitation has ion-pair nature. So, in the 3–4.5 Å

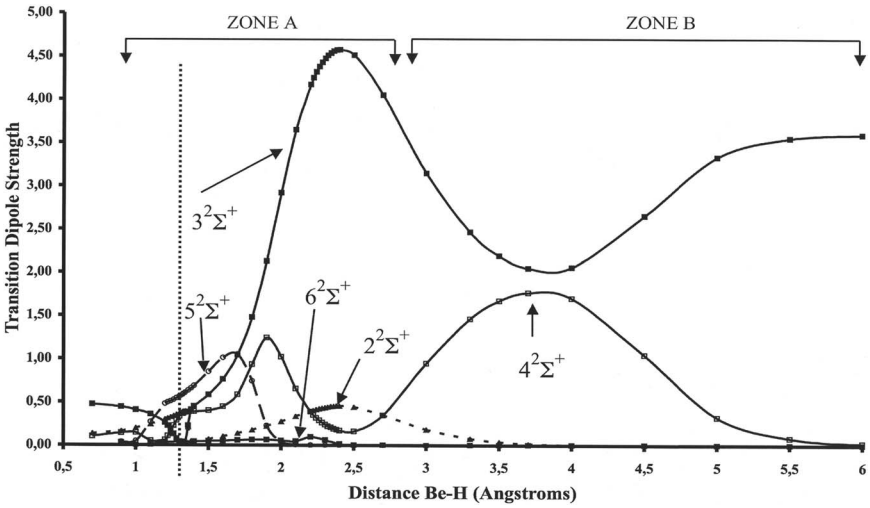

FIG. 7. Transition dipole strength, $|\langle \mathrm{exc}|\hat{\mu}|0\rangle|^2$ (in a.u.), for $^2\Sigma^+ \leftarrow X\,^2\Sigma^+$ transitions as a function of the internuclear distance for BeH.

range, where the ion-pair is more relevant in the description of the $3\,^2\Sigma^+$ state, its TDS distinctly falls. Consistently, no appreciable values of TDS are calculated for the $5\,^2\Sigma^+$ or $6\,^2\Sigma^+$ states for $R=8$ Å, in a region where the ion-pair dominate these states (see Fig. 3).

As concerns the TDS to $^2\Pi$ states (Fig. 8), except for the $A\,^2\Pi$ state that presents a quasilineal decreasing tendency, the remaining $^2\Pi$ states show a more complex behavior. The $2\,^2\Pi$ state does show a short zone of steepest change among 1.7–1.8 Å, where its TDS value sharply increases up to the atomic limit. This just occurs in the region where this state suffers an important avoided crossing as explained in Sec. III C.

The double-well nature of the $4\,^2\Pi$ potential energy curve is also reflected in the behavior of the TDS at this distance range (1.3–1.7 Å). Together with the $5\,^2\Pi$ state, the TDS suffers several changes, local maxima and minima, at this range.

As mentioned above, the states that dissociate to $\mathrm{Be}(^1P)+\mathrm{H}(^2S)$ have high TDS at large R. Instead, the TDS of the $4\,^2\Pi$ state that can be described as the $(4p)$ Rydberg state at short distances falls to zero as R increases. This state dissociate to $\mathrm{Be}(^3P)+\mathrm{H}(^2S)$, and it should imply a spin forbidden transition in the closed-shell Be atom.

The R_e of the GS is indicated with a dotted vertical line in Figs. 7 and 8. The $A\,^2\Pi(\mathrm{val})$ and $5\,^2\Sigma^+$ states have the greatest TDSs there. The oscillator strengths (OS), as get from the TDS values, are reported in Table VII (the OS for the $\Pi \leftarrow \Sigma$ transitions include a factor of 2). The good agreement that was obtained with a shorter basis set[67] with the OS values of the MRD-CI calculations by Bruna and Grein[108] is found again. Finally, let us recall that the largest OS among the $^2\Sigma^+$ states comes from the $5\,^2\Sigma^+(3d)$ state, that, as already discussed by Clerbaux and Colin[41] may contribute to observations of the D state of BeH, while the $6\,^2\Sigma^+(4s)$ state is found at a higher energy than the D complex and has a very low TDS associated to the transition from the GS, indicating that this should be a very weak transition.

IV. CONCLUSIONS

We present in this work FCI calculations of the adiabatic potential curves of the lower excited states of the BeH molecule with a valence ANO basis set augmented with a one-center ANO Rydberg set. The first six $^2\Sigma^+$, the first five $^2\Pi$, the first two $^2\Delta$, and the first $^2\Sigma^-$ states have been calculated. Also, the first $^4\Sigma^+$ and $^4\Pi$ states have been obtained. The curves have been calculated in great detail so that its numerous features provide benchmark references for calculations that must account for different physical situations such as,

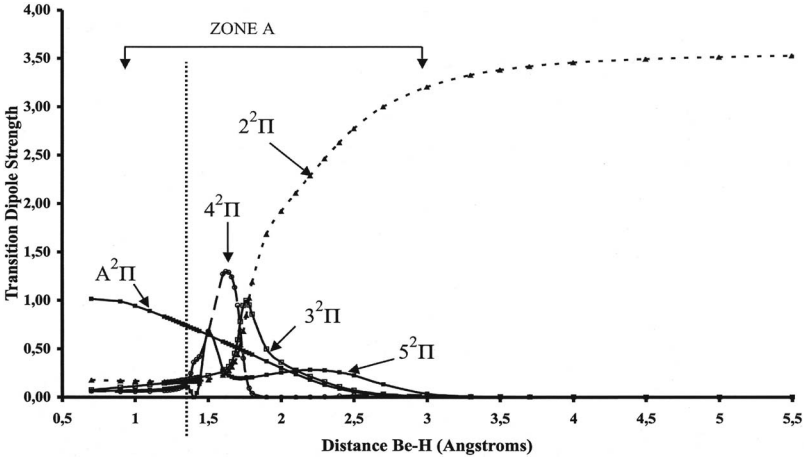

FIG. 8. The y component of the electric transition dipole strength, $|\langle \mathrm{exc}|\hat{\mu}_y|0\rangle|^2$ (in a.u.), for the $^2\Pi \leftarrow X\,^2\Sigma^+$ transitions as a function of the internuclear distance for BeH.

e.g., Rydberg-valence interactions, ion-pair and neutral state interactions, multistate avoided crossings, diexcited states, or multiconfigurational wave functions.

The adiabatic curves that can be related to the vertical $n=3$ Rydberg states [$3\,^2\Sigma^+(3s)$, $4\,^2\Sigma^+(3p)$, $5\,^2\Sigma^+(3d)$, $2\,^2\Pi(3p)$, $3\,^2\Pi(3d)$ and $1\,^2\Delta(3d)$] and two valence states ($C\,^2\Sigma^+$ and $A\,^2\Pi$) have been described. Information concerning other states [mainly the $6\,^2\Sigma^+(4s)$, $4\,^2\Pi(4p)$, $5\,^2\Pi(4d)$, and $2\,^2\Delta(4d)$] has been also obtained in a more limited way.

A well balanced calculation of the valence-Rydberg mixing and an appropriated accounting of the $(2\sigma)^{-1}\rightarrow(3\sigma)^{+1}$ contribution are required to reproduce the shape of the curves of the $^2\Sigma^+$ states. At short distances, valence-Rydberg mixing is involved in the short-extent avoided crossings and, in particular, in that one between the 2 and $3\,^2\Sigma^+$ states near 1.4 Å. On other hand, at large distances, the ion-pair nature of the states is involved in the perturbation, and the most notorious case is the long-extent avoided crossing between the $3\,^2\Sigma^+$ and $4\,^2\Sigma^+$ states at 4–5 Å.

Some spectroscopic parameters have been calculated from the vibrational states that result from the adiabatic curves assuming uncoupled vibration and rotation in all cases. In spite of this assumption, that is rough for some states as, e.g., the D complex, the spectroscopic parameters obtained help to assess the reliability of our calculations and confirm some of previous works on BeH. Notwithstanding, an exhaustive comparison with actual experimental data should require to take into account nonadiabatic coupling in most cases and falls out of the scope of the present work. For some states (as for example, the $B\,^2\Pi$ and $G\,^2\Pi$ states), these couplings can have important consequences when comparing with the experimental reported results. According to the picture that draws the present FCI adiabatic curves, there is no evidence of a $^2\Pi$ state with a $R_e=1.925$ Å that experimentally has been described as the $G\,^2\Pi$ state. However, the double-well nature of the $4\,^2\Pi$ potential curve is confirmed by the interaction of the nearby $^2\Pi$ states.

Concerning the remaining states, the present FCI calculations contribute to explain some details and to confirm previously suggested explanations of other authors. The absence of the $3s$ and $3p\,^2\Sigma^+$ states in the absorption spectrum can surely be due to the predissociative interaction with the $C\,^2\Sigma^+$ state in terms of the perturbation of the vibration levels.

In this work we have discussed that some vibrational states could be populated in the $4\,^2\Sigma^+(3p)$ state at distances around the minimum located at about 4.169 Å that results from the avoided crossing with the $3\,^2\Sigma^+(3s)$ state. Such vibrational states would occur in the Born–Oppenheimer regime and would imply changes in electronic nature (covalent and ion pair) along each vibration. A few spectroscopic parameters have been calculated for this minimum. A note of caution is still convenient here to recall that all the parameters shown and discussed in the present study refer to the adiabatic energy potentials.

It is possible to resolve the so-called "D complex" into three different states ($5\,^2\Sigma^+$, $3\,^2\Pi$, and $1\,^2\Delta$) whose adiabatic T_e values should differ in less than 180 cm^{-1}. It must also be pointed out the nonexistence of a double minimum in the $2\,^2\Pi(3p)$ state, in spite of the strong multistate avoided crossing occurring at about 1.7–1.9 Å, as confirmed by our FCI calculations, in agreement with the conclusions of Machado *et al.* for this state[52] and contrarily to the interpretations of Colin and co-workers for the $B\,^2\Pi$ state.[36,37,41]

On the other hand, the controversy about the assignment of the E and $F\,^2\Sigma^+$ states is reopened. The 6 and $7\,^2\Sigma^+$ states that can be assigned as $4s$ and $4p$ Rydberg states, respectively, do not match with the experimental excitation energies. Moreover, only one $^2\Sigma^+$ state is found at about 54 100 cm^{-1}, the $5\,^2\Sigma^+(3d)$ state. The TDS calculations show that the only relevant oscillator strength contribution to the transitions close to 54 100 cm^{-1} associated to $^2\Sigma^+$ states comes from the $5\,^2\Sigma^+(3d)$ state. The next $^2\Sigma^+$ state, namely, the $6\,^2\Sigma^+$ state, is high in energy by $\sim$2200–2300 cm^{-1} above the D complex region, and should present a very weak transition.

The analysis of the evolution of the DM and the TDS with the internuclear distance R is of great help to locate the position of the avoided crossings, to show their extent along a short or long interval of R values, and to reveal the number of states implied in them, as well as their strength.

ACKNOWLEDGMENTS

The present work has been supported by European FEDER funds and Spanish project MEC (CTQ2007-67143-C02/BOU) and GV (GVAINF2007-051). J.P.R. acknowledges the Spanish project MEC+FEDER (CTQ2004-01739/BQU). A.M.V. also wishes to acknowledge her research agreement awarded, with the "Ramon y Cajal" program, by the Spanish MEC and FSE. The authors are indebted to Dr. S. Evangelisti (University of Toulouse, France) and Dr. G.L. Bendazzoli (Universita di Bologna, Italy), for the revised versions of the VEGA code.

[1] *Modern Electronic Structure Theory*, edited by D. R. Yarkony (World Scientific, Singapore, 1995), Parts I and II.
[2] *Recent Advances in Coupled-Cluster Methods*, edited by R. J. Bartlett (World Scientific, Singapore, 1997).
[3] J. Paldus and X. Li, Adv. Chem. Phys. **110**, 1 (1999), and references therein.
[4] *Recent Advances in Multireference Methods*, edited by K. Hirao (World Scientific, Singapore, 1999).
[5] G. F. Bauerfeldt and H. Lischka, J. Phys. Chem. A **108**, 3111 (2004).
[6] D. P. Schofield and H. G. Kjaergaard, J. Chem. Phys. **120**, 6930 (2004).
[7] X. Z. Yang, M. R. Lin, and B. Z. Zhang, J. Chem. Phys. **120**, 7470 (2004).
[8] W. Eisfeld, J. Chem. Phys. **120**, 6056 (2004).
[9] J. Pitarch-Ruiz, S. Evangelisti, and D. Maynau, Int. J. Quantum Chem. **97**, 688 (2004).
[10] D. Walter, A. Venkatnathan, and E. A. Carter, J. Chem. Phys. **118**, 8127 (2003).
[11] A. I. Krylov, Chem. Phys. Lett. **350**, 522 (2001).
[12] H. A. Witek, H. Nakano, and K. Hirao, J. Chem. Phys. **118**, 8197 (2003).
[13] C. Angeli, S. Borini, and R. Cimiraglia, Theor. Chem. Acc. **111**, 352 (2004).
[14] Y. G. Khait, J. Song, and M. R. Hoffmann, J. Chem. Phys. **117**, 4133 (2002).
[15] R. K. Chaudhuri, K. F. Freed, G. Hose, P. Piecuch, K. Kowalski, M. Wloch, S. Chattopadhyay, D. Mukherjee, Z. Rolik, A. Szabados, G. Tóth, and P. R. Surján, J. Chem. Phys. **122**, 134105 (2005).
[16] I. S. O. Pimienta, K. Kowalski, and P. Piecuch, J. Chem. Phys. **119**, 2951 (2003).
[17] S. Li, J. Ma, and Y. Yiang, J. Chem. Phys. **118**, 5736 (2003).
[18] J. Pittner, J. Chem. Phys. **118**, 10876 (2003).

[19] M. Kállay, P. G. Szalay, and P. R. Surján, J. Chem. Phys. **117**, 980 (2002).
[20] L. Adamowicz, J. P. Malrieu, and V. V. Ivanov, J. Chem. Phys. **112**, 10075 (2000).
[21] U. S. Mahapatra, B. Datta, and D. Mukherjee, Mol. Phys. **94**, 157 (1998).
[22] T. Fang and S. Li, J. Chem. Phys. **127**, 204108 (2007).
[23] F. A. Evangelista, W. D. Allen, and H. F. Schaefer III, J. Chem. Phys. **125**, 154113 (2006).
[24] J. Paldus, in *Methods in Computational Molecular Physics*, NATO ASI Series B: Physics, edited by S. Wilson and G. H. F. Diercksen (Plenum, New York, 1992), Vol. 293, pp. 99–194; in *Relativistic and Electron Correlation Effects in Molecules and Solids*, NATO ASI Series B: Physics, edited by G. L. Malli (Plenum, New York, 1994), Vol. 318, pp. 207–282.
[25] X. Li and J. Paldus, J. Chem. Phys. **104**, 9555 (1996).
[26] H. Meissner and J. Paldus, J. Chem. Phys. **113**, 2622 (2000).
[27] D. Mukherjee and S. Pal, Adv. Quantum Chem. **20**, 292 (1989).
[28] P. G. Szalay and J. Gauss, J. Chem. Phys. **112**, 4027 (2000).
[29] D. Maurice and M. Head-Gordon, J. Phys. Chem. **100**, 6131 (1996).
[30] M. Head-Gordon, D. Maurice, and M. Oumi, Chem. Phys. Lett. **246**, 114 (1995).
[31] J. Guan, M. E. Casida, and D. R. Salahub, J. Mol. Struct.: THEOCHEM **527**, 229 (2000).
[32] T. Kobayashi, K. Sasagane, and K. Yamaguchi, Int. J. Quantum Chem. **65**, 665 (1997).
[33] S. Budavari, M. J. O'Neil, A. Smith, and P. E. Heckelman, *The Merck Index*, 11th ed. (Merck, New Jersey, 1989), pp. 181–183.
[34] R. Horne and R. Colin, Bull. Soc. Chim. Belg. **81**, 93 (1972).
[35] D. De Greef and R. Colin, J. Mol. Spectrosc. **53**, 455 (1974).
[36] R. Colin and D. De Greef, Can. J. Phys. **53**, 2142 (1975).
[37] R. Colin, C. Drèze, and M. Steinhauer, Can. J. Phys. **61**, 641 (1983).
[38] R. Colin and M. Steinhauer, Bull. Soc. Chim. Belg. **92**, 507 (1983).
[39] C. Focsa, S. Firth, P. F. Bernath, and R. Colin, J. Chem. Phys. **109**, 5795 (1998).
[40] R. Colin, D. De Greef, P. Goethals, and G. Verhaegen, Chem. Phys. Lett. **25**, 70 (1974).
[41] C. Clerbaux and R. Colin, Mol. Phys. **72**, 471 (1991).
[42] A. Shayesteh, K. Tereszchuk, P. F. Bernath, and R. Colin, J. Chem. Phys. **118**, 1158 (2003).
[43] C. Focsa, S. Firth, P. F. Bernath, and R. Colin, J. Chem. Phys. **109**, 5795 (1998).
[44] C. Focsa, P. F. Bernath, R. Mitzner, and R. Colin, J. Mol. Spectrosc. **192**, 348 (1998).
[45] R. J. Le Roy, D. R. T. Appadoo, R. Colin, and P. F. Bernath, J. Mol. Spectrosc. **236**, 178 (2006).
[46] NIST Chemistry WebBook, NIST Standard Reference Database Number 69, edited by P. J. Linstrom and W. G. Mallard, June 2005, National Institute of Standards and Technology, Gaithersburg MD, 20899 (http://webbook.nist.gov).
[47] C. Henriet and G. Verhaegen, Phys. Scr. **33**, 299 (1986).
[48] I. D. Petsalakis, G. Theodorakopoulos, and C. A. Nicolaides, J. Chem. Phys. **97**, 7623 (1992).
[49] P. S. Bagus, C. M. Moser, P. Goethals, and G. Verhaegen, J. Chem. Phys. **58**, 1886 (1973).
[50] D. L. Cooper, J. Chem. Phys. **80**, 1961 (1984).
[51] J. M. L. Martin, Chem. Phys. Lett. **283**, 283 (1998).
[52] F. B. C. Machado, O. Roberto-Neto, and F. R. Ornellas, Chem. Phys. Lett. **284**, 293 (1998).
[53] I. D. Petsalakis, D. Papadopoulos, G. Theodorakopoulos, and R. J. Buenker, J. Phys. B **32**, 3225 (1999).
[54] R. Martinazzo, A. Famulari, M. Raimondi, E. Bodo, and F. A. Gianturco, J. Chem. Phys. **115**, 2917 (2001).
[55] G. Gerratt and M. Raimondi, Proc. R. Soc. London, Ser. A **371**, 525 (1980).
[56] D. L. Cooper, J. Chem. Phys. **80**, 1961 (1984).
[57] M. Larsson, J. Chem. Phys. **81**, 6409 (1984).
[58] M. Larsson, Phys. Scr. **32**, 97 (1985).
[59] X. Li and J. Paldus, J. Chem. Phys. **102**, 2013 (1995).
[60] R. S. Mulliken, Int. J. Quantum Chem., Symp. **5**, 95 (1971).
[61] J. Paldus and J. Cizek, J. Chem. Phys. **52**, 2919 (1970).
[62] G. Corongiu, J. Phys. Chem. A **110**, 11584 (2006).
[63] H. Lefebvre-Brion and R. Colin, J. Mol. Spectrosc. **65**, 33 (1977).
[64] I. D. Petsalakis, R. J. Buenker, G. Hirsh, and G. Theodorakopoulos, J. Phys. B **30**, 4935 (1997).
[65] M. P. Fülscher and L. Serrano-Andres, Mol. Phys. **100**, 903 (2002).
[66] S. Bubin and L. Adamowicz, J. Chem. Phys. **126**, 214305 (2007).
[67] J. Pitarch-Ruiz, J. Sánchez-Marín, and A. M. Velasco, J. Comput. Chem. **29**, 523 (2008).
[68] P. O. Widmark, P. A. Malmqvist, and B. O. Roos, Theor. Chim. Acta **77**, 291 (1990).
[69] B. O. Roos, M. Fülscher, P. A. Malmqvist, M. Merchán, and L. Serrano-Andrés, *Theoretical Studies of the Electronic Spectra of Organic Molecules, in Quantum Mechanical Electronic Structure Calculations with Chemical Accuracy*, edited by S. R. Langhoff (Kluwer Academic, Dordrecht, The Netherlands, 1995), pp. 357–431, and references therein.
[70] K. Kaufmann, W. Baumeister, and M. Jungen, J. Phys. B **22**, 2223 (1989).
[71] I. Martín, C. Lavín, Y. Pérez-Delgado, J. Pitarch-Ruiz, and J. Sánchez-Marín, J. Phys. Chem. A **105**, 9637 (2001).
[72] J. Pitarch-Ruiz, J. Sánchez-Marín, I. Martín, and A. M. Velasco, J. Phys. Chem. A **106**, 6508 (2002).
[73] A. M. Velasco, I. Martín, J. Pitarch-Ruiz, and J. Sánchez-Marín, J. Phys. Chem. A **108**, 6724 (2004).
[74] A. M. Velasco, J. Pitarch-Ruiz, Alfredo M. J. Sánchez de Merás, J. Sánchez-Marín, and I. Martín, J. Chem. Phys. **124**, 124313 (2006).
[75] J. Pitarch-Ruiz, E. Mayor, A. M. Velasco, A. Sánchez de Merás, J. Sánchez-Marín, and I. Martín, J. Phys. Chem. A **111**, 3321 (2007).
[76] T. H. Dunning, Jr., J. Chem. Phys. **90**, 1007 (1989).
[77] Extension with respect to the cc-pVTZ basis set was retrieved from the EMSL public database: Basis Set Exchange v1.1: A Community Database for Computational Sciences; K. L. Schuchardt, B. T. Didier, T. Elsethagen, L. Sun, V. Gurumoorthi, J. Chase, J. Li, and T. L. Windus, J. Chem. Inf. Model. **47**, 1045 (2007).
[78] A. J. Sadlej, Theor. Chim. Acta **79**, 123 (1991).
[79] A. J. Sadlej and M. Urban, J. Mol. Struct.: THEOCHEM **80**, 147 (1991).
[80] K. Andersson, M. Barysz, A. Bernhardsson, *et al.*, MOLCAS, version 5.4, Lund University, Sweeden, 2002.
[81] G. L. Bendazzoli and S. Evangelisti, J. Chem. Phys. **98**, 3141 (1993).
[82] G. L. Bendazzoli and S. Evangelisti, Int. J. Quantum Chem., Quantum Chem. Symp. **27**, 287 (1993).
[83] J. M. Junquera-Hernández, J. Sánchez-Marín, G. L. Bendazzoli, and S. Evangelisti, J. Chem. Phys. **121**, 7103 (2004).
[84] D. Maynau, MOLCOST program, University of Toulouse, France, 2003.
[85] C. Angeli, G. L. Bendazzoli, S. Borini, R. Cimiraglia, A. Emerson, S. Evangelisti, D. Maynau, A. Monari, E. Rossi, J. Sanchez-Marín, P. G. Szalay, and A. Tajti, Int. J. Quantum Chem. **107**, 2082 (2007).
[86] S. Borini, A. Monari, E. Rossi, A. Tajti, C. Angeli, G. L. Bendazzoli, R. Cimiraglia, A. Emerson, S. Evangelisti, D. Maynau, J. Sanchez-Marin, and P. G. Szalay, J. Chem. Inf. Model. **47**, 1271 (2007).
[87] E. Rossi, A. Emerson, and S. Evangelisti, Lect. Notes Comput. Sci. **316**, 2658 (2003).
[88] A. Monari, G. L. Bendazzoli, S. Evangelisti, C. Angeli, N. Ben Amor, S. Borini, D. Maynau, and E. Rossi, J. Chem. Theory Comput. **3**, 477 (2007).
[89] MATHEMATICA 5.2 Wolfram Research, http://www.wolfram.co.uk
[90] J. M. Hutson, J. Phys. B: Atomic and Molec. Phys. **14**, 851 (1981).
[91] J. M. Hutson, CDIST, a program for calculating centrifugal distortion constants for diatomic molecules. Quantum Chemistry Program Exchange Bulletin 2, 33 (1982) QCPE-435.
[92] R. J. Le Roy, LEVEL 8.0, a computer program for solving the radial Schrödinger equation for bound and quasibound levels, University of Waterloo Chemical Physics Research Report CP-663, 2007; see http://leroy.uwaterloo.ca/programs/
[93] K. P. Huber and G. Herzberg, *Molecular Spectra and Molecular Structure: Constants of Diatomic Molecules* (Van Nostrand, Toronto, 1979), Vol. IV.
[94] J. M. Hollas, *High Resolution Spectroscopy*, 2nd ed. (Wiley, Chichester, 1998).
[95] M. Molsky, J. Phys. Chem. A **103**, 5269 (1999).
[96] R. Rydberg, Z. Phys. **73**, 376 (1931).
[97] J. N. Murrell and K. S. Sorbie, J. Chem. Soc., Faraday Trans. 2 **70**, 1552 (1974).
[98] Ch.-L. Yang, X. Zhang, and K.-L. Han, J. Mol. Struct.: THEOCHEM **676**, 209 (2004).
[99] J. L. Dunham, Phys. Rev. **41**, 721 (1932).
[100] J. N. Murrell, S. Carter, S. C. Farantos, P. Huxley, and A. J. C. Varandas, *Molecular Potential Energy Functions* (Wiley, Chichester, 1984).

[101] E. Wigner and E. E. Witmer, Z. Phys. **51**, 859 (1928).
[102] A. E. Kramida and W. C. Martin, J. Phys. Chem. Ref. Data **26**, 1185 (1997).
[103] K. R. Lykke, K. K. Murray, and W. C. Lineberger, Phys. Rev. A **43**, 6104 (1991).
[104] D. E. Woon and T. H. Dunning, Jr., J. Chem. Phys. **100**, 2975 (1994); See also EMSL public database given in Ref. 77 for some of the augmented exponents.
[105] P. E. Cade, R. F. W. Bader, and J. Pelletier, J. Chem. Phys. **54**, 3517 (1971).
[106] H. E. Popkie, J. Chem. Phys. **54**, 4597 (1971).
[107] W. H. Henneker and H. E. Popkie, J. Chem. Phys. **54**, 1763 (1971).
[108] P. J. Bruna and F. Grein, Phys. Chem. Chem. Phys. **5**, 3140 (2003).
[109] A. C. H. Chan and E. R. Davidson, J. Chem. Phys. **49**, 727 (1968).
[110] K. P. Huber and G. Herzberg, *Constants of Diatomic Molecules in NIST Chemistry WebBook*, NIST Standard Reference Database, edited by W. G. Mallard and P. J. Linstrom (National Institute of Standards and Technology, Gaithersburg, MD, 1999), No. 69; http://webbook.nist.gov
[111] W. W. Watson, Phys. Rev. **32**, 600 (1928).
[112] W. W. Watson and A. E. Parker, Phys. Rev. **37**, 167 (1931).
[113] E. Olsson, Z. Phys. **73**, 732 (1932).
[114] P. G. Koontz, Phys. Rev. **48**, 707 (1935).
[115] See EPAPS Document No. E-JCPSA6-129-626828 for data files associated with this paper. For more information on EPAPS, see http://www.aip.org/pubservs/epaps.html.
[116] L. D. Landau, Phys. Z. Sowjetunion **2**, 46 (1932).
[117] C. Zener, Proc. R. Soc. London, Ser. A **137**, 696 (1932).
[118] E. E. Whiting, A. Schadee, J. B. Tatum, J. T. Hougen, and R. W. Nichols, J. Mol. Spectrosc. **80**, 249 (1980).
[119] V. S. Gurin, M. V. Korolkov, V. E. Matulis, and S. K. Rakhmanov, J. Chem. Phys. **126**, 124321 (2007).
[120] M. V. Korolkov and K.-M. Wietzel, J. Chem. Phys. **123**, 164308 (2005).